Landscape and Urban Planning 168 (2017) 94–116

Contents lists available at ScienceDirect

Landscape and Urban Planning

journal homepage: www.elsevier.com/locate/landurbplan

Research Paper

A future land use simulation model (FLUS) for simulating multiple land use scenarios by coupling human and natural effects

Xiaoping Liu[a], Xun Liang[a], Xia Li[b,a,*], Xiaocong Xu[a,*], Jinpei Ou[a], Yimin Chen[b,a], Shaoying Li[c], Shaojian Wang[a], Fengsong Pei[d]

[a] Guangdong Key Laboratory for Urbanization and Geo-simulation, School of Geography and Planning, Sun Yat-sen University, Guangzhou, 510275, PR China
[b] School of Geographic Sciences, Key Lab. of Geographic Information Science (Ministry of Education), East China Normal University, 500 Dongchuan Rd, Shanghai 200241, PR China
[c] School of Geographical Sciences, Guangzhou University,Guangzhou, Guangdong, PR China
[d] School of Geography, Geomatics, and Planning, Jiangsu Normal University, Xuzhou, 221116, Jiangsu, China

ARTICLE INFO

Keywords:
Land use and land cover change
Land use simulation
System dynamics
Cellular automata
FLUS
Human and natural effects

ABSTRACT

Land use and land cover change (LUCC) simulation models are effective and reproducible tools for analyzing both the causes and consequences of future landscape dynamics under various scenarios. Current simulation models primarily focus on the evolution of specific land use types under the influence of human activities, but they rarely consider background climatic effects. However, these background climate changes significantly affect the landscape dynamics and should be incorporated into long-term LUCC simulations under various human-climate-included scenarios. In this paper, we propose a future land use simulation (FLUS) model that explicitly simulates the long-term spatial trajectories of multiple LUCCs. The top-down system dynamics and bottom-up cellular automata were interactively coupled during the projection period, which improved the model's ability to accurately simulate future land use patterns. A self-adaptive inertia and competition mechanism was developed within the CA model to process the complex competitions and interactions between the different land use types. The proposed model was applied to an LUCC simulation in China from 2000 to 2010. The results show promising grid-to-grid agreement compared to actual land use, and the simulation accuracy is higher than other well-accepted models, such as CLUE-S and CA models. The model was further applied to the simulation of four scenarios from 2010 to 2050 that depict different development strategies by considering various socio-economic and natural climatic factors. The simulation results and findings demonstrate that the proposed model is effective for future LUCC simulation under variously designed scenarios. FLUS is available for free download at http://www.geosimulation.cn/FLUS.html.

1. Introduction

The land cover on earth and its anthropogenic exploitation are crucial links between human activities and the natural environment. Since the industrial era, land use and land cover change (LUCC) has been critical in contributing to regional and global climate change by driving energy recycling and material exchange on the land surface (Foley et al., 2005). Human-involved LUCCs, such as forest over-exploitation, agricultural intensification and urbanization, not only accelerate global warming via increasing greenhouse gas emissions (Kalnay & Cai, 2003; Pielke et al., 2002) but also pervasively cause irreversible biological diversity losses across the globe (Matson, Parton, Power, & Swift, 1997; Tilman et al., 2001; Vitousek, Mooney, Lubchenco, & Melillo, 1997). Rapid urban expansion and socio-economic development have increased the tension in human-environment interactions (Vitousek et al., 1997; Yao et al., 2016), as more than 50% of the world's population lived in urban areas in 2007, a number that will likely reach approximately 70% by 2050 (Bloom, 2011).

Spatiotemporal LUCC simulations are effective and reproducible tools for analyzing both the causes and consequences of alternative future landscape dynamics relative to socio-economic and natural environmental driving forces (Costanza & Ruth, 1998; Verburg, Schot, Dijst, & Veldkamp, 2004). The complex structure of linkages and feedback is expected to be solved using simulation models to project future land use trajectories and support future land-use policy decisions (Heistermann, Müller, & Ronneberger, 2006; Kline, Moses, Lettman, & Azuma, 2007; Schulp, Nabuurs, & Verburg, 2008). Cellular automata (CA) are common methods to simulate the LUCC spatial

* Corresponding authors.
E-mail addresses: liuxp3@mail.sysu.edu.cn (X. Liu), liangxunnice@163.com (X. Liang), lixia@geo.ecnu.edu.cn, lixia@mail.sysu.edu.cn (X. Li), xuxiaoc@mail3.sysu.edu.cn (X. Xu).

http://dx.doi.org/10.1016/j.landurbplan.2017.09.019
Received 8 July 2016; Received in revised form 2 September 2017; Accepted 17 September 2017

evolution by estimating the state of a pixel according to its initial state, the surrounding neighborhood effects and a set of transition rules. Although very simple, a CA model can generate rich patterns and can effectively represent nonlinear spatially stochastic LUCC processes (Batty, Couclelis, & Eichen, 1997). In the last two decades, a growing body of literature has described the applications of CA models in urban development studies (Clarke & Gaydos, 1998; Li and Yeh, 2000,2002; Li, Chen, Liu, Li, & He, 2011; White, Engelen, & Uljee, 1997; Wu, 1999). By properly defining the transition rules, urban CA models have strong capabilities for simulating the spatiotemporal complexities of urban systems (Chen, Li, Wang, & Liu, 2012; Li, Lin, Chen, Liu, & Ai, 2013; Liu & Hu et al., 2017; Liu, Li, Liu, He, & Ai, 2008; Liu, Li, Shi, Wu, & Liu, 2008; Liu, Li, Shi, Zhang, & Chen, 2010; Liu et al., 2014). Other studies have focused on simulating deforestation under the influences of natural hazards or human activities (Gustafson, Shifley, Mladenoff, Nimerfro, & He, 2000; Kok & Winograd, 2002). However, most of these models can only simulate the dynamics of one individual land use, while in many cases, different LUCC processes occur simultaneously and affect each other. Thus, multiple LUCC simulations are much more effective for determining realistic future land use patterns. Conducting multiple LUCC simulations within one CA model is challenging because of the interaction and competition among different land uses, which inevitably leads to very complicated definitions of the transition rules. The complicated interactions and competition among different land use types are not well explored. Most current studies simply estimate the probabilities of individual land use types separately and assign the highest value to the land grid, such as the ANN-CA (Li & Yeh, 2002) and CLUE-S series models (Verburg et al., 2002; Verburg & Overmars, 2009). Moreover, the role of climate change in long-term land use patterns is not well addressed in these models.

Climate change (global warming, extreme weather events, etc.) and ecological degradation (hydrological variation, soil erosion, etc.) have long-term effects that alter the natural landscape dynamics (Bakker et al., 2005; Geist & Lambin, 2004; Lambin, Geist, & Lepers, 2003; Li, Guangzhao, Xiaoping, & Xun, 2017; Okin, Murray, & Schlesinger, 2001). Temperature variability, freshwater availability and soil quality affect various human-dominated land use decisions, such as the redistribution and transformation of cultivated land, grassland and pastureland (Mendelsohn & Dinar, 1999; Wolf, Bindraban, Luijten, & Vleeshouwers, 2003). Such interactions and feedback within the LUCC environmental system will eventually have profound impacts on human welfare and long-term social sustainability through air pollution, natural resource shortages, food risk, etc. (Hansen, 2010; Hay & Mimura, 2006). Issues such as land degradation (De Koning, Verburg, Veldkamp, & Fresco, 1999), biodiversity (Chapin et al., 2000; Sala et al., 2000) and global climate change (Tangen, 1999) have increasingly demanded quantitative information on regional and global LUCCs and their future changes, both spatially and temporally. The exploration of both the LUCC natural environmental and anthropogenic impacts is vitally important for climate change adaptation and maintaining a sustainable landscape.

Another challenge of multiple LUCC simulations is that CA models are bottom-up models that determine the system evolution from a local perspective. However, macro-scale demands, political planning and background climate influences on different land use types cannot be properly represented in the traditional CA models (Ward, Murray, & Phinn, 2000). Thus, it is necessary to introduce top-down models to address these planning and development factors, such that demands for different use types can be determined from the macro-scale perspective and can be regarded as scenarios that represent future development pathways (Sohl, Sayler, Drummond, & Loveland, 2007; Xiang & Clarke, 2016). Through such coupling, the land use change quantities can be rationally determined. Subsequently, the CA model iterates and allocates these land use change quantities according to the transition rules at the local level. A series of researchers have proposed models to integrate the top-down quantitative estimation methods, such as historical trend extrapolation, complex multi-sector models (Verburg & Overmars, 2009), Forrester models (Berling-Wolff & Wu, 2004), and system dynamics (He et al., 2005; Huang, He, Liu, & Shi, 2014), using the bottom-up CA model to better simulate the LUCC dynamics. These top-down methods are designed to address the demands, planning, and developments of individual land use types from a macro-scale perspective to determine the land use change quantities. The CA model then allocates these land use change quantities through local interactions and evolutions of different land use types at the grid cell level. Examples of such integrated CA models include CLUE-S (Verburg et al., 2002), LTM (Pijanowski, Alexandridis, & Mueller, 2006), the SLEUTH model (Dietzel & Clarke, 2007), and FORE-SCE (Sohl et al., 2007). However, problems still occur, because these coupled models directly link two sub-models via the land use demands at the end of the study period, despite the bottom-up and top-down models being built using different assumptions. The interactions and feedback loops between the bottom-up and top-down models are ignored, leading to the separation of the macro land use demand projections and the local change allocations.

Although many of these models have addressed socio-economic and geographic condition factors, few studies have considered the background climate conditions. Many previous studies (Bakker et al., 2005; Mendelsohn & Dinar, 1999; Wolf et al., 2003) have agreed that climate factors (e.g., temperature increases and precipitation variations) have significant effects on specific LUCCs, such as forest, farmland, and pastureland. Without incorporating climate change scenarios, these models are not applicable for future LUCC simulations under human-climate-included scenarios and are therefore unable to reliably determine future land use patterns due to the significant effects of climate change on the LUCC dynamics. In addition, the top-down and bottom-up models are typically built upon different assumptions. Current simulation models typically loosely integrate two sub-models via the land use demands at the end of the study period, but they seldom consider their interactions and feedback, leading to the separation of the macro land use demand projection and the local change allocation. To summarize, although great progress has been achieved, three limitations exist in the current multiple LUCC simulation models: 1) Although the socio-economic factors and geographic conditions are well addressed, few studies have considered the background climate conditions. Future climate changes will have significant impacts on the long-term land use dynamics. 2) Most of the multiple LUCC models train and estimate the conversion probabilities of each land use type independently, resulting in a separation between the different land use types. The competition and interactions are not well explored in these models. Finally, 3) the interactions and feedback between the top-down and bottom-up models are not typically coupled, which results in the separation between the macro land use demand projection and the local change allocation.

In this paper, we present an approach that interactively integrates top-down system dynamics (SD) with a bottom-up CA model for a multiple LUCC dynamic simulation. The proposed integrated model differs from existing models in its ability to explicitly simulate the spatial trajectories of multiple LUCCs under alternative scenarios by coupling both human-related and natural environmental effects using an elaborate design of the interactions and competition among different land use types and using an interactive coupling mechanism between the SD and CA models. In the proposed model, we incorporated natural factors, including future global warming and precipitation variations and socio-economic developments into both the SD and CA models. A self-adaptive inertia and competition mechanism is designed to address the complex local land use interactions and estimate the transition probabilities of different land use types simultaneously. An “interactive coupling” mechanism is introduced into the model allocation, which integrates the bottom-up and top-down models interactively via the mutual feedbacks between land use quantities and local allocations along the entire simulated time series. This new coupling mechanism enables the two sub-models to evolve collaboratively. The proposed

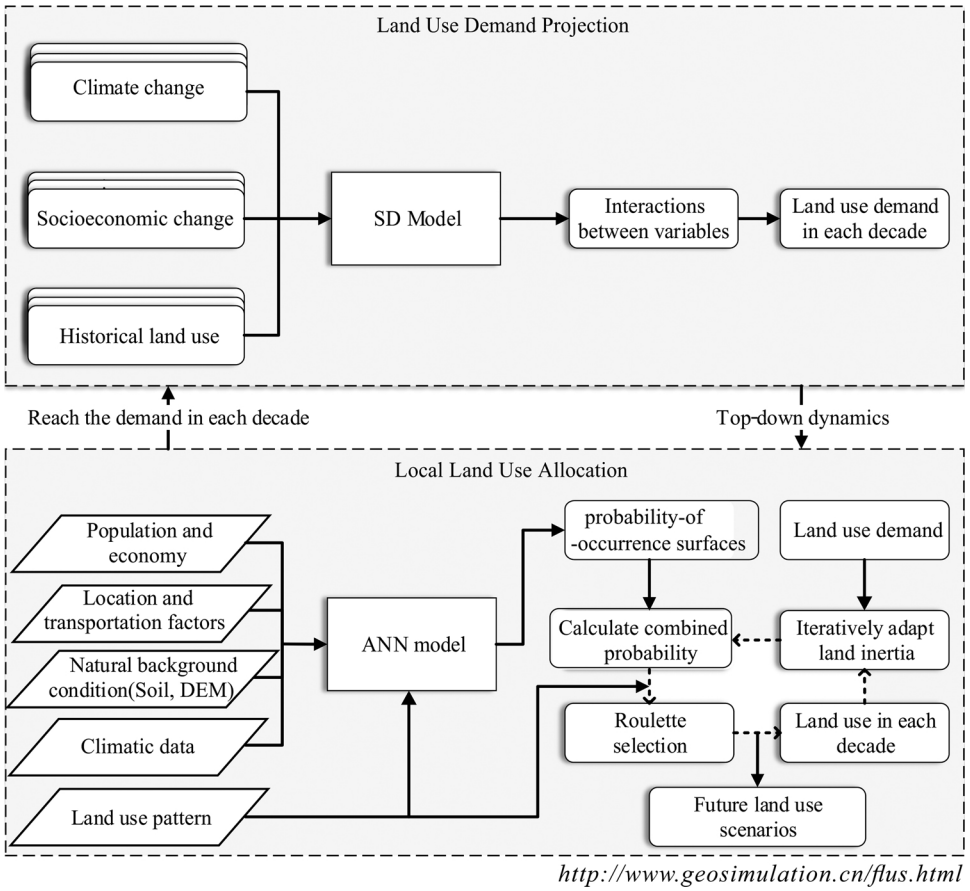

Fig. 1. The framework of the proposed FLUS model.

model is illustrated with multiple LUCC simulation scenarios in the China region from 2010 to 2050 at a spatial resolution of 1 × 1 km^2. Four scenarios were designed based on the impacts of both the natural environment and human activities. The simulation results are compared and analyzed to assess the human and natural effects on future LUCCs.

2. Methodology

In this paper, we present a future land use simulation (FLUS) model for multiple LUCC scenarios for future land use by coupling human and natural effects. The proposed model is an integration of a top-down system dynamic (SD) model and bottom-up cellular automata (CA). The SD model is used to project the land use scenario demands under various socio-economic and natural environmental driving factors at the national/regional scale. A self-adaptive inertia and competition mechanism is developed within the CA model to process the complex competitions and interactions among the different land use types. The general structure of the FLUS model is illustrated in Fig. 1.

2.1. Land use demand projection using system dynamics (SD)

The SD model is an effective approach for modeling the nonlinear behavior of complex systems over time by using stocks, flows, internal feedback loops and time delays (Coyle, 1997). It can be used to understand and predict the evolution of a complex system through the feedback and interactions among different elements. Currently, the SD model is widely used in policy making and analysis throughout the public and private sectors (Costanza & Ruth, 1998; Haghani, Lee, & Byun, 2003).

In this study, we developed an SD model to project the multiple land use demands under different scenarios by considering both human activities and natural ecological effects. The interactions and feedback of the developed SD model are presented in Fig. 2. The developed SD model consists of four sectors: population, economy, climate and land use. The population sector is essential, since it will cause consequential variations in the other sectors. The economy sector has strong influences on population and land use, as GDP (gross domestic product) affects the change in the fixed-asset investments, thereby driving the economic investment in various land use types. As mentioned above, the background climate conditions have a long-term effect on altering the natural landscape dynamics; thus, the climate sector (annual precipitation and temperature) is also included in the SD model. Variations in temperature are assumed to have various influences on the growth and regeneration capacity of cultivated land, forest land and grassland. Similarly, appropriate increases in precipitation are sufficient to meet the water requirements of vegetation, leading to changes in cultivated land, forest land and grassland. In total, six land use types are considered in the land use sector: urban land, cultivated land, grassland, forest, water area and unused land. The changes in each land use type are constrained by the integrated influences of socio-economic and climate conditions as well as by the interactions among the various land use types. For example, urban land is estimated by multiplying the urban population by the GDP value, which directly affects the changes in cultivated land and water area. Moreover, the forest and grassland areas are estimated by the socio-economic factors and climate conditions, such as precipitation and temperature. This SD component provides a convenient way to capture the major impacts of the socio-economic and climate changes on the land use demands in China.

2.2. Land use change simulation using cellular automata (CA)

The multiple CA allocation model is developed to simulate the future spatial pattern under the given land use demands determined by the SD model. The CA simulation is implemented in two steps: 1) an

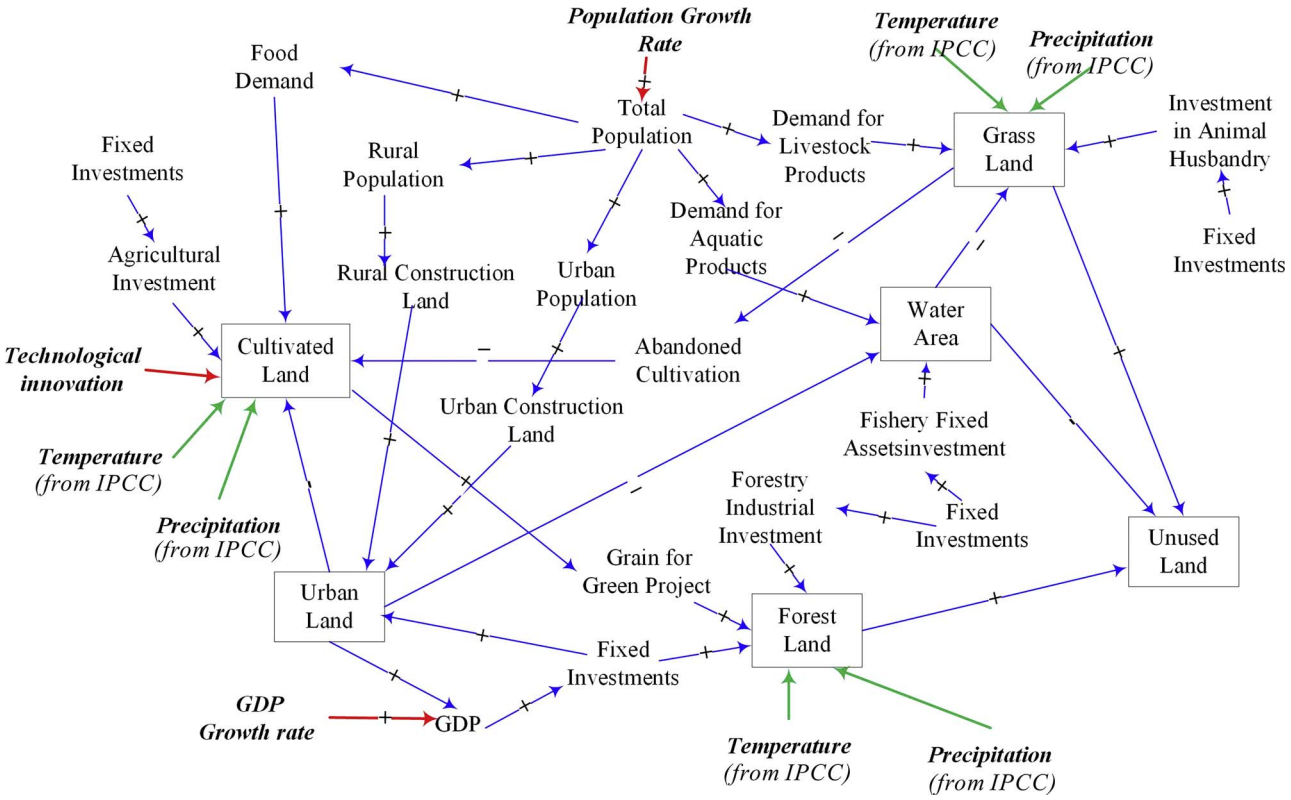

Fig. 2. The interactions and competition of different land use types driven by human and natural factors in the system dynamics.

artificial neural network is used to train and estimate the probability-of-occurrence of each land use type on a specific grid cell, and 2) an elaborate self-adaptive inertia and competition mechanism is designed to address the competition and interactions among the different land use types. Through these two steps, the combined probabilities of all the land use types at each specific grid cell are estimated, and the dominant land use type is allocated to this grid cell during the CA iteration. In the allocation process, a specific land grid either retains the current land use type or transforms into another type depending on their combined probabilities and the roulette selection (as described in detail below). A schematic framework of the CA allocation model is presented in Fig. 3.

2.2.1. Probability-of-occurrence estimation using artificial neural networks

Artificial neural networks (ANNs) are a family of machine learning models inspired by biological neural networks (e.g., the human brain) and are typically used to estimate or approximate non-linear functions that are dependent on many inputs (independent variables). The advantage of ANNs is that they are capable of learning and fitting complex relationships between input data and training targets through a number of learning-recall iterations (Li & Yeh, 2002). ANNs have been successfully applied to the analysis and modeling of various non-linear geographical problems (Openshaw, 1998). It is well accepted that ANNs are able to achieve promising performance when modeling a large number of inputs and outputs (Wang, 1994).

In general, an ANN with multiple input and output neurons consists of three layer types: an input layer, a hidden layer and an output layer (Fig. 4). In the input layer, each neuron corresponds to an input variable, e.g., independent spatial variables, socio-economic variables and natural climate variables in the CA model. It can be mathematically expressed as

$$X = [x_1, x_2, \ldots, x_n]^T \quad (1)$$

where $x_i$is the i th neuron in the input layer. In the hidden layer, the signal received by neuron j from all the input neurons on grid cell p at time t is estimated according to the following equation:

$$net_j(p, t) = \sum_i w_{i,j} \times x_i(p, t) \quad (2)$$

where $net_i(p, t)$ is the signal received by neuron j in the hidden layer; $x_i(p, t)$ is the ith variable associated with the input neuron i on grid cell p at training time t; and $w_{i,j}$ is an adaptive weight between the input layer and the hidden layer, which is calibrated during the training process. The connection between the hidden layer and the output layer is determined by an activation function. The sigmoid activation function is effective for building the connection between the hidden layer and the output layer, which is estimated as follows:

$$\text{sigmoid}(net_j(\text{p, t})) = \frac{1}{1 + e^{-net_j(p,t)}} \quad (3)$$

Each neuron in the output layer corresponds to a specific land use type. The value of the lth neuron in the output layer will generate a value that represents the probability-of-occurrence for the lth land use type at the grid cell. A higher value indicates that the specific grid cell has a higher probability-of-occurrence for the target land use type. The probability-of-occurrence of land use type k on grid cell p at training time t is denoted as $P(p, k, t)$ and is estimated according to the following equation:

$$\text{p(p,k,t)} = \sum_j w_{j,k} \times sigmoid(net_j(p, t)) = \sum_j w_{j,k} \times \frac{1}{1 + e^{-net_j(p,t)}} \quad (4)$$

where $w_{j,k}$ is an adaptive weight between the hidden layer and the output layer, and similar to $w_{i,j}$, it is calibrated during the training process. After both $w_{i,j}$ and $w_{j,k}$ are trained and calibrated using the training dataset, the ANN model is built and can be used to estimate the probability-of-occurrence for each land use type in a specific grid cell.

2.2.2. Self-adaptive inertia and competition mechanism

The ANN model was developed to establish the relationship between the probability-of-occurrence surface for a specific land use type

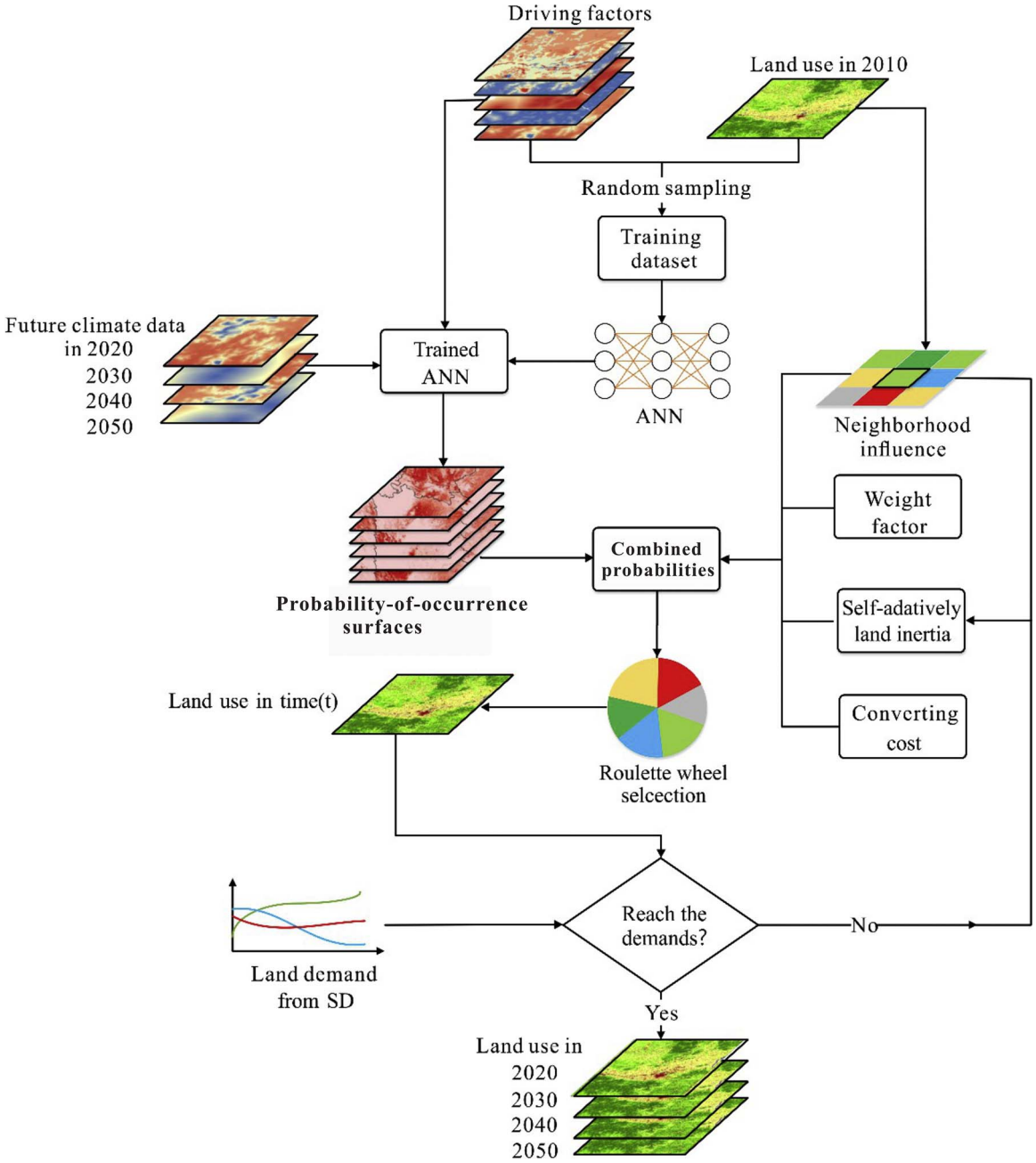

Fig. 3. The schematic framework of the Cellular Automata (CA) local allocation.

and the given spatial factors. Similar to previous large-scale simulation models, such as CLUE-S (Verburg, Schulp, Witte, & Veldkamp, 2006), LUS (Letourneau, Verburg, & Stehfest, 2012), and CLUMondo (Van Asselen & Verburg, 2013), this relationship is assumed to remain relatively unchanged over the study period due to the essential nature of the land use. Whether a land grid will be developed into a specific land use type depends not only on the probability-of-occurrence but also on other variable components accounting for different development statuses over the prediction period. Thus, in the proposed model, we incorporate the probability-of-occurrence with the conversion cost, neighborhood condition and competition among the different land use types to estimate the combined probability for each land grid. Moreover, the interactive coupling of the top-down SD demand and the bottom-up CA model enhances the model's capability for long-term simulation.

2.2.2.1. Neighborhood effects. The neighborhood development density effect considered in this study is similar to that of traditional CA models. At a specific grid cell p, the neighborhood development density for land use type k is defined as

$$\Omega_{p,k}^{t} = \frac{\sum_{N\times N} con(c_p^{t-1} = k)}{N \times N - 1} \times w_k \quad (5)$$

In this equation, $\sum_{N\times N} con(c_p^{t-1} = k)$ represents the total number of grid cells occupied by the land use type k at the last iteration time $t - 1$ within the $N \times N$ window. w_k is the variable weight among the different land use types because there are different neighborhood effects for different land use types. The neighborhood weight value for each land use type is determined based on expert knowledge and a series of model tests. The final neighborhood weight for each land use type is illustrated in Table 3.

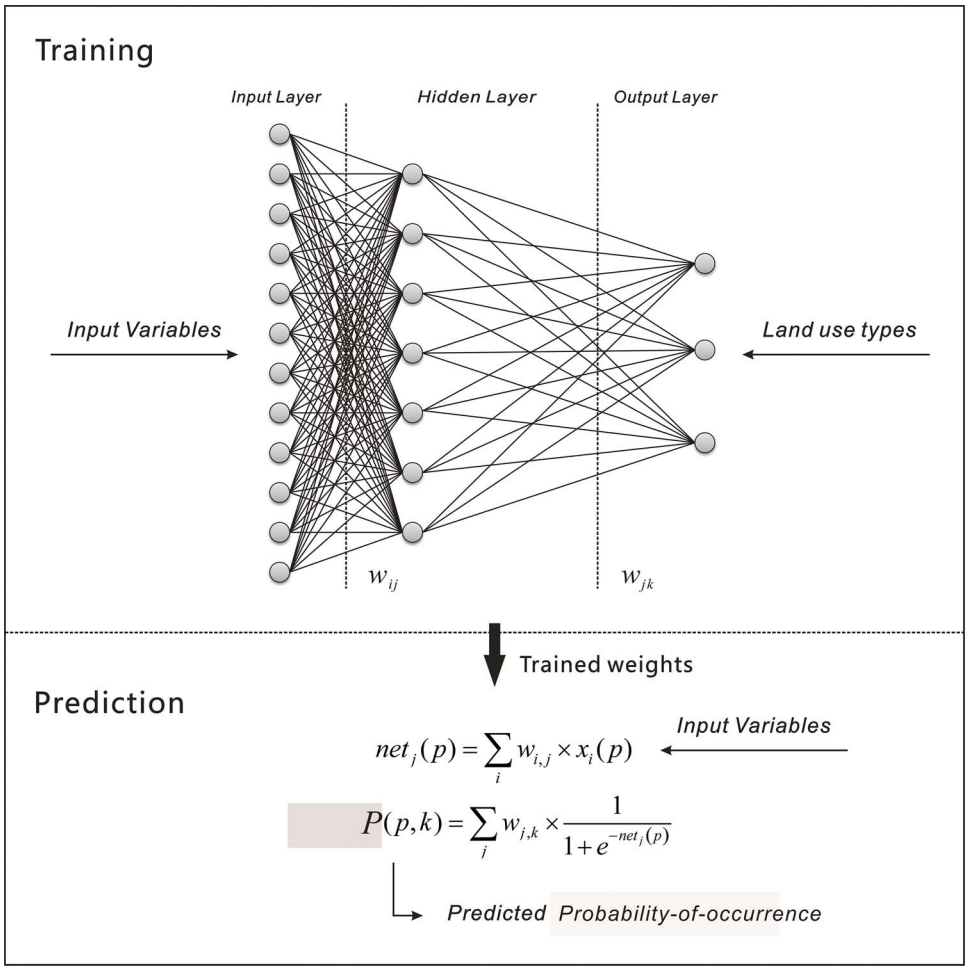

Fig. 4. Basic structure of an artificial neural network with multiple inputs and outputs.

2.2.2.2. Inertia coefficient. The most important factor in the proposed model involves the competition and interaction of different land use types during the multiple CA evolution iterations. A self-adaptive inertia should be used to represent the inheritance of previous land use types. A self-adaptive inertia coefficient for each land use type is thus defined to auto-adjust the inheritance of the current land uses on each grid cell according to the differences between the macro demand and the allocated land use amount. The core idea is that if the developing trend of a specific land use type contradicts the macro demand, the inertia coefficient would dynamically increase the inheritance of this land use type to rectify the land use trajectory in the next iteration. For example, if future planning requires more cultivated land, whereas the allocation of the cultivated land decreases in the last iteration, the inertia coefficient will increase to preserve additional cultivated land and to promote the conversion of other land use types to cultivated land. The inertia coefficient is defined as:

$$\text{Intertia}_k^t = \begin{cases} \text{Intertia}_k^{t-1} & \text{if } |D_k^{t-1}| \le |D_k^{t-2}| \\ \text{Intertia}_k^{t-1} \times \frac{D_k^{t-2}}{D_k^{t-1}} & \text{if } D_k^{t-1} < D_k^{t-2} < 0 \\ \text{Intertia}_k^{t-1} \times \frac{D_k^{t-1}}{D_k^{t-2}} & \text{if } 0 < D_k^{t-2} < D_k^{t-1} \end{cases} \quad (6)$$

where $Inertia_k^t$ denotes the inertia coefficient for land use type k at iteration time t. D_k^{t-1} denotes the difference between the macro demand and the allocated amount of land use type k until iteration time $t-1$. Note that the inertia coefficient is defined with respect to the current land use type occupying the grid cell. Thus, if the considered land use type k is not the current land use, then the inertia coefficient of land use type k will be set to 1, and it will not alter the combined probability of land use type k for this grid cell. According to Eq. (6), the inertia coefficient is defined based on three different situations: 1) If the developing trend of the specific land use type k meets the macro demand, i.e., $|D_k^{t-2}| \le |D_k^{t-1}|$, then the inertia coefficient at iteration time t will remain unchanged. 2) If the macro demand for the specific land use type k is less than the current allocation amount, and the developing trend of land use type k contradicts the macro demand, i.e. , then the inertia coefficient at iteration time t will decrease slightly by multiplying the previous coefficient by D_k^{t-2}/D_k^{t-1}. 3) If the macro demand for the specific land use type k is greater than the current allocation amount and the developing trend of land use type k contradicts the macro demand, i.e., $0 < D_k^{t-2} < D_k^{t-1}$, then the inertia coefficient at iteration time t will increase slightly by multiplying the previous coefficient by D_k^{t-1}/D_k^{t-2}. Through the dynamic tuning of the inertia coefficients for all land use types in the CA iteration, the allocations of different land use types compete with each other, resulting in a scenario where all the land use allocations match the macro land use demands.

2.2.2.3. Conversion cost. The conversion cost, which indicates the conversion difficulty from the current land use type to the target type, is another factor shaping the land use dynamics (Aerts & Heuvelink, 2002; Huang, Liu, Li, Liang, & He, 2013). Similar parameters analogous to the conversion cost have been used in some large-scale LUCC simulation models, such as the CLUE-S (Verburg et al., 2002), FORE_SCE (Sohl & Sayler, 2008), and CLUMondo (Van Asselen & Verburg, 2013) models. These models predefine a group of static experience-based parameters for a specific region that denotes the

Table 1
Conversion cost of land use pairs.

Land use types	Cultivated land	Forest land	Grass land	Water area	Urban land	Unused land
Cultivated land	0	0.9	0.1	0.8	0.1	0.4
Forest land	0.7	0	0.3	0.99	0.99	0.8
Grass land	0.5	0.8	0	0.4	0.3	0.1
Water area	0.9	0.9	0.9	0	0.99	0.5
Urban land	1	1	1	1	0	1
Unused land	0.9	0.99	0.5	0.8	0.3	0

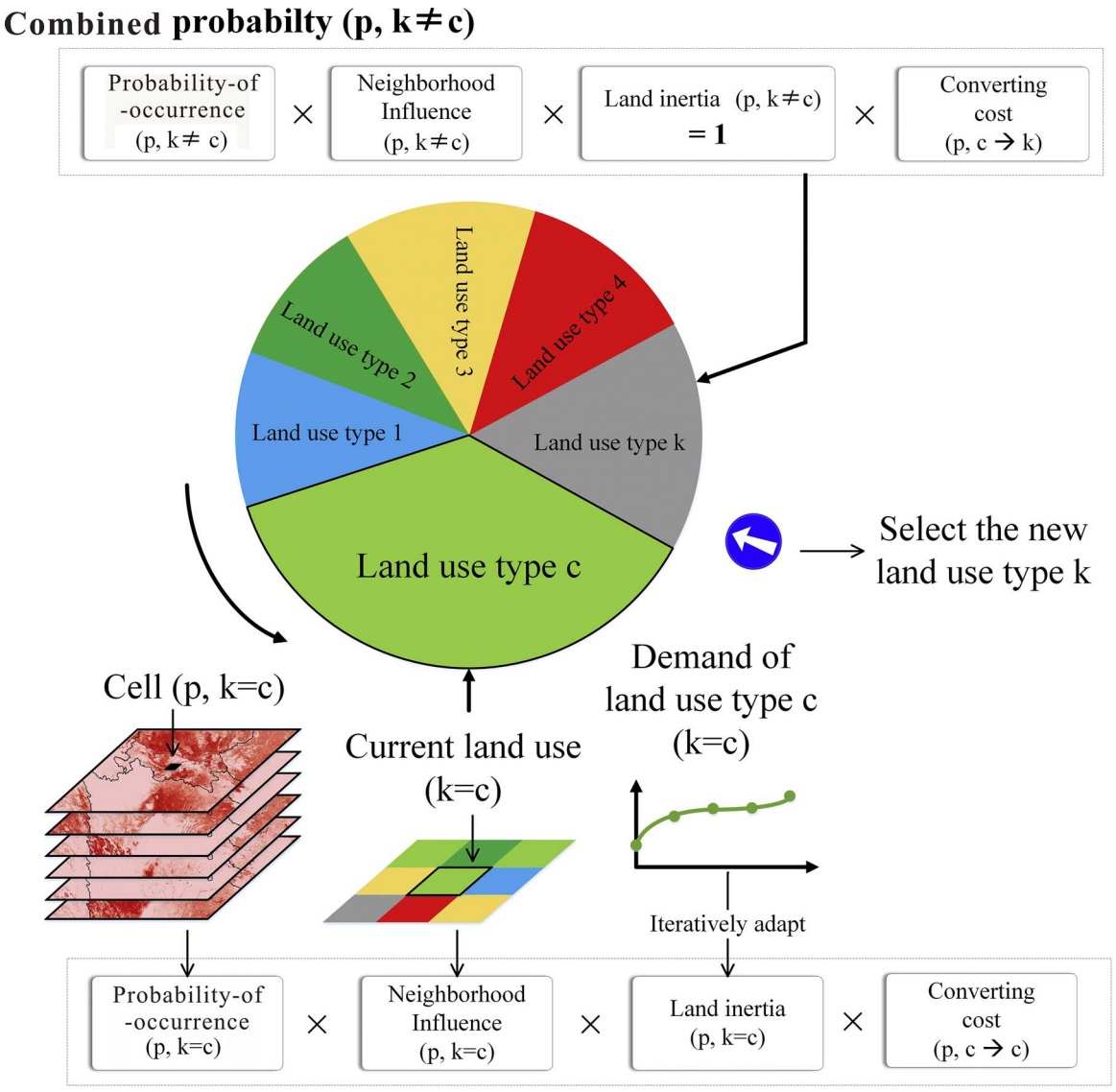

Fig. 5. Schematic diagram of the roulette selection mechanism.

conversion difficulty.

The conversion cost defined in this paper is a brief summary of the difficulty for a specific land grid to change from one land use type to another. It is estimated based on an analysis of the historical land use data in the study area and regional expert opinions. It reflects the intrinsic attributes of land uses without considering the changeable influences, such as technological progress and human activities. Thus, the conversion cost remains unchanged in the proposed model. Other changeable factors are reflected by the neighborhood effects, the inertia coefficient and the interactive integration with the system dynamic model, which will continue to vary over the study period. The conversion costs are different for individual land use types. For example, the cost of converting urban land into grassland is relatively high, while the cost of converting agricultural land to urban construction land is relatively low. For each land use pair c and k, the cost of the land use change from c to k is denoted as $sc_{c\to k}$. In this study, the conversion cost of each land use pair is determined based on local expert experience and urban planners (Table 1). The value of the conversion cost $sc_{c\to k}$ varies between the range of [0,1]. Larger values indicate a greater conversion difficulty, and a value of 1 means that the conversion is nearly impossible. We have also developed a sensitivity analysis for testing the model sensitivity to conversion cost in Section 4.

2.2.2.4. Roulette selection. By considering the probability-of-

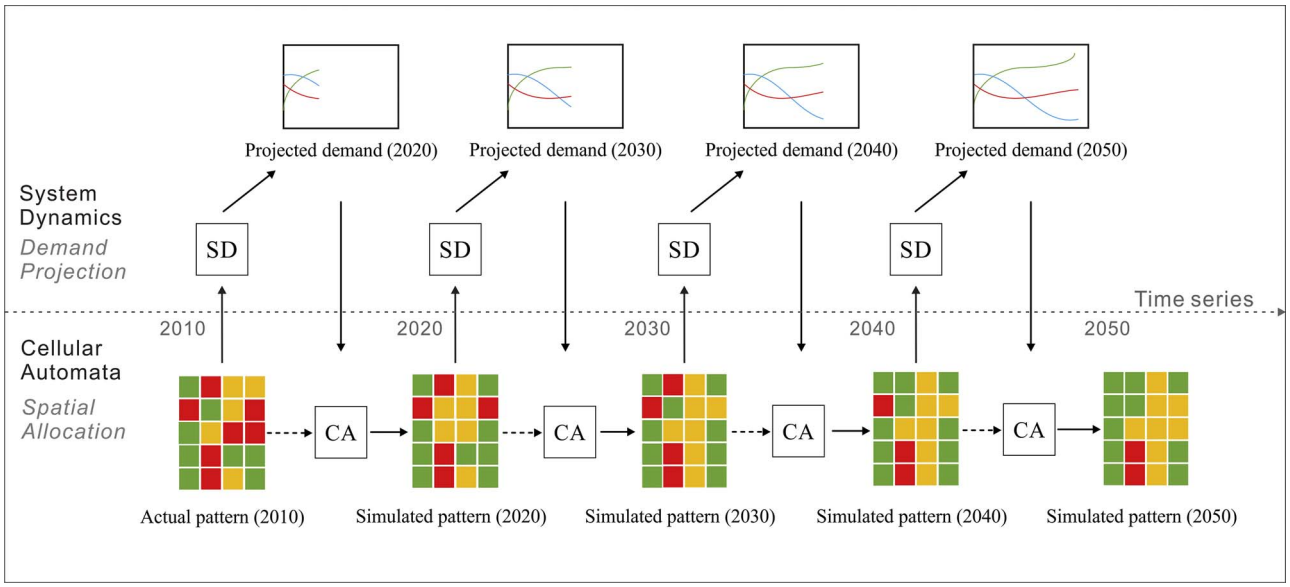

Fig. 6. Interactive coupling mechanism of the SD model and multiple CA model.

occurrence, neighborhood effect, inertia coefficient and conversion cost, the combined probability of a cell being occupied by a specific land use type is estimated using the following equation:

$$TP_{p,k}^{t} = P_{p,k} \times \Omega_{p,k}^{t} \times Inertia_{k}^{t} \times (1 - sc_{c \to k}) \quad (7)$$

where $TP_{p,k}^{t}$ denotes the combined probability of grid cell p to covert from the original land use type to the target type k at iteration time t; $P_{p,k}$ denotes the probability-of-occurrence of land use type k on grid cell p; $\Omega_{p,k}^{t}$ denotes the neighborhood effect of land use type k on grid cell p at iteration time t; $inertia_{k}^{t}$ denotes the inertia coefficient of land use type k at iteration time t; and $sc_{c \to k}$ denotes the conversion cost from the original land use type c to the target type k.

After estimating the combined probability for each iteration time, the CA simulation will determine whether a grid cell is converted or not. If it is converted, the simulation will determine which land use type will occupy the grid cell in the next iteration. In most previous models, such as CLUE-S, the land use type of a specific grid cell is simply allocated to the dominant cell with the highest conversion probability (Verburg et al., 2002). Other studies used pre-defined thresholds to control the conversion rate by comparing the highest conversion probability and the threshold (Li & Yeh, 2002). These methods only consider the dominant land use type and disregard the competition with other land use types, thereby eliminating allocation opportunities for non-dominant land use types.

Undoubtedly, the dominant land use type with the highest combined probability is the priority for grid cell allocation, but the other land use types with relatively lower combined probabilities still have a chance to be allocated, even though the chances are small. To achieve this, we propose the use of a roulette selection mechanism to determine which land use type will occupy the grid cell. The probability of a land use being allocated is proportional to its combined probability. A schematic diagram of the roulette selection mechanism is shown in Fig. 5. For a specific grid cell p at iteration time t, the combined probability of each land use type is estimated according to Eq. (7), after which a roulette wheel is constructed according to the combined probabilities of all the land use types. Each sector of the roulette wheel is represented by a land use type. The area of a sector is proportional to its combined probability. Then, a uniformly distributed random number ranging from 0 to 1 is generated, and based on the associated sector of the random number, the corresponding land use type is allocated to the grid cell in the current iteration. Through this roulette selection mechanism, a land use type with a higher combined probability is more likely to be selected as the occupying land use, and those with relatively lower combined probabilities still have a chance to be allocated. In addition, the stochastic characteristics of this mechanism enable the model to reflect the uncertainty of real-world LUCC dynamics, extending its applicability to the leapfrog-grown land use simulations.

2.3. Integration of the SD model with the multiple CA model

In the proposed FLUS model, the top-down SD demand projection model and the bottom-up CA local allocation model are not loosely coupled via the final land use demands as with many integrated models. Instead, analogous to Syphard's study (Syphard, Clarke, & Franklin, 2007), they are interactively (tightly) coupled through individual land use quantities during the study time series. To strengthen the mutual feedback between the SD and CA sub-models, the study period was divided into several intervals during which these two sub-models evolved collaboratively. The projected land use demand derived from the SD model in the previous time node was used as an input for the CA model to simulate the land use pattern in the current time node, and this simulation, together with other driving factors, was used to project the land use demand to the next time node using the SD model. This input-output mutual feedback continues and finally generates the land use pattern at the end of the simulation period.

A schematic diagram of the coupling mechanism is illustrated in Fig. 6. We use the period of 2010–2050 as an example to explain the coupling mechanism. The 40-year period was divided into four intervals: 2010–-2020, 2020–2030, 2030–2040, and 2040–2050. At the beginning and end of each time interval, the SD and CA models would exchange input/output information. The demand of all the land use types in 2020 is projected through the configured SD model using the actual land use pattern in 2010 and the influence of both human and natural factors during this time interval. Then, the trained multiple CA model simulates the local competition and interactions iteratively and generates the land use pattern in 2020, which meets the projected demand derived from the SD model. Subsequently, a newly configured SD model adjusted by the simulated land use pattern in 2020 is used as a feedback to project the demand for 2030. Then, the CA model sequentially simulates the land use pattern from 2020 to 2030. The mutual feedback between the SD model and CA model continues and, finally, collaboratively generates the land use pattern in 2050 for different scenarios. Based on this interactive coupling approach, we developed the GeoSOS-FLUS software as an extension to our previous

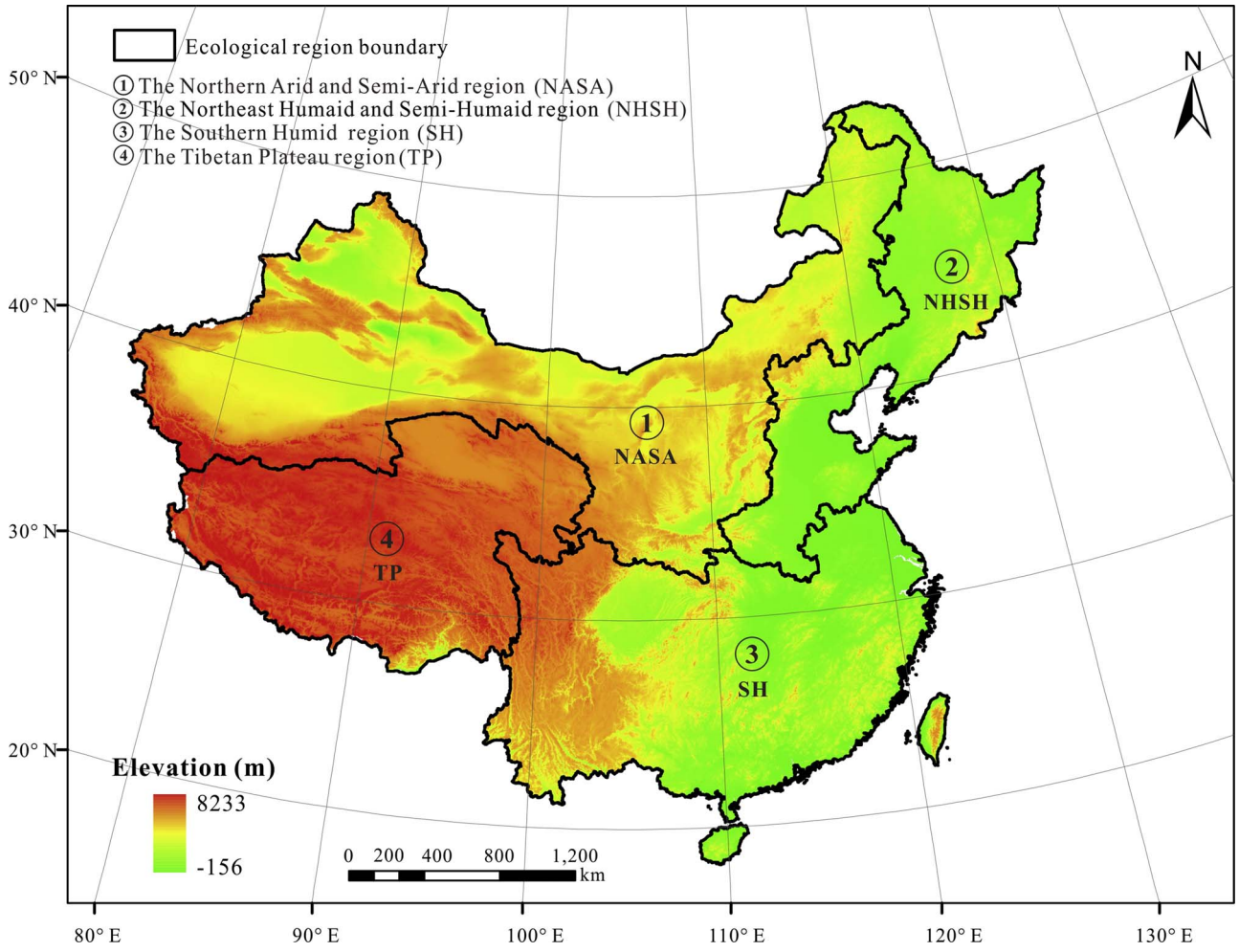

Fig. 7. Study area and the four divided ecological regions.

GeoSOS software (Li et al., 2011) to facilitate the multiple land use change simulations under human-natural-included scenarios (available for free download at http://www.geosimulation.cn/flus.html).

3. Land use simulations for mainland China during 2000–2010

The applicability of the proposed FLUS model was first tested by LUCC simulations of mainland China during 2000–2010. China is the second largest country in the world, covering an area of 9.6 million square kilometers with various landscape patterns. In the past two decades, China has undergone significant urban expansion due to its rapid economic development and population increases, and significant urbanization processes are expected to continue in the coming decades (Chen, Liu, & Tao, 2013). It is very important for decision-makers to predict future land use changes under different planning scenarios and to evaluate the influences of both human activities and climate change on the LUCC dynamics.

3.1. Data preparation and model configuration

Considering the significant differences regarding the climate and ecosystem characteristics across the vast region of mainland China, we divided the study area into four major ecological regions (Fu, Liu, Chen, Ma, & Li, 2001) (Fig. 7): the northeast humid and semi-humid (NHSH) region, the northern arid and semi-arid (NASA) region, the southern humid (SH) region, and the Tibetan Plateau (TP) region. The spatial dataset used to build and train the proposed model is listed in Table 2, including historical and current land use patterns, terrain conditions (elevation and slope), socio-economic and positional data (population, GDP, city site and road network), climatic and ecological factors (soil quality, temperature and precipitation) and future climate variations. All of the spatial datasets were resampled to the same resolution of $1 \times 1\ km^2$.

The application of the FLUS model in China includes six land use types: cultivated land, forest land, grassland, water area, urban land and unused (barren) land (including sandy land, Gobi, salina, swampland, bare soil, bare rock, alpine desert and tundra). A total of 15 spatial driving factors that were derived from the original datasets listed in Table 2 and normalized to the range of [0,1] were selected to establish the ANN model for the probability-of-occurrence estimation for each land use type. The ANN model is designed to have 15 neurons in the input layer (corresponding to 15 spatial driving factors) and 6 neurons in the output layer (corresponding to 6 land use types). The log-sigmoid function is selected as the model transfer function to ensure the estimated probability values fall within [0,1]. The mean square error (MSE) is used as the objective function in the back-propagation (BP) training process. The training process stops when the MSE is less than 0.001. In the FLUS model, we used the 5×5 extended Moore neighborhood to represent the neighborhood space. The neighborhood weights for individual land use types in different ecological regions are illustrated in Table 3. The initial inertia coefficients for the first iteration are set to 1 for all land use types and will subsequently evolve according to Eq. (6) during the CA iteration.

Table 2
List of data used in this study.

Category	Data	Year	Resolution	Data resource
Land use	Land use data	2000–2010	30m	CAS (http://www.resdc.cn)
Human influence	Population	2010	0.5′	LandScan 2010 Global Population Project
	GDP	2010	1 km	CAS (http://www.resdc.cn)
	City site	2014	1 km	World Urbanization Prospects: The 2014 Revision, CD-ROM Edition.
	Road network	2010	1 km	NASA, Socioeconomic Data and Applications Center, Global Roads Open Access Data Set (gROADS), v1
Terrain	DEM	2000	0.5′	WorldClim version 1.4 (http://www.worldclim.org/)
	Slope	2000	0.5′	Calculated from DEM
Soil	Nutrient availability Oxygen availability to roots Excess salts. Workability	2008	5′	Har monized World Soil Database v 1.2 (http://webarchive.iiasa.ac.at/Research/LUC/External-World-soil-database/HTML/SoilQuality.html?sb=10)
Climate	Annual Mean Temperature Temperature Seasonality Temperature Annual Range Annual Precipitation Precipitation Seasonality	2000	0.5′	WorldClim version 1.4 (http://www.worldclim.org/)
Future Climate	Annual Mean Temperature Annual Precipitation	2010–2050	0.5°	World Data Climate Center (http://cera-www.dkrz.de/WDCC/)
Subarea	Ecological Zones	2001	Vector	Fu et al. (2001)

3.2. Model implementation and validations

The applicability of the proposed model was tested by simulating future LUCCs in China. A total of 500 thousand samples were randomly selected across the Chinese territory; 70% of the samples (training set) were used to train the model, and the remaining 30% (validation set) were used to quantitatively assess its performance. The demands of the six land use types in 2010 were projected using the SD model (http://vensim.com/vensim-software/) based on the land use pattern in 2000 as well as the socio-economic factors and environmental tendencies from 2000 to 2010. The spatial evolution of multiple land uses from 2000 to 2010 was subsequently simulated to meet the given land use demands derived from the SD model. The FLUS model performance is assessed based on three aspects: the fit of the ANN model to the probability-of-occurrence, the agreement between the simulation result and the actual land use pattern, and a comparison with the current simulation models.

3.2.1. Validation of ANN performance

The Receiver Operating Characteristic (ROC) curve and the Area Under ROC Curve (AUC) values (Hanley & McNeil, 1982) were used to quantify the ANN model performance in terms of fitting the individual land use probability-of-occurrence. The ROC is an effective tool for illustrating the performance of a binary classifier system, due to its variable discrimination threshold. The ROC curve is created by plotting the true positive rate (TPR, known as the *sensitivity* in machine learning) against the false positive rate (FPR, estimated with $1 - specificity$) at various threshold selections. A larger area under the ROC curve (AUC value) corresponds to a better model fitting performance. Generally, a completely random model yields an AUC value of 0.5, and a perfectly fitting result yields an AUC value of 1.0. Fig. 8 shows the ROC curves of six land use types in red and the random guess curves in green. The AUC values of each land use type were estimated according to the ROC curves. We found that the AUC values of cultivated land, grassland and water area were larger than 0.8, and the AUC values of the forest land, urban land and unused land were greater than 0.9. Such promising AUC values indicate that the probability-of-occurrence fit for the individual land uses can be well explained by the selected driving factors.

3.2.2. Comparison with other studies

The spatial land use simulation in 2010 and the actual land use pattern of 2010 are shown in Fig. 9, with three partial enlargements to display more details of the simulated results. The figure shows that the simulated pattern is well correlated with the actual pattern at the national scale. The enlarged views of three select regions also show high spatial consistencies for the six land use types. To quantitatively assess the simulated result, samples in the test set were used to build the grid-by-grid confusion matrix of the simulated result versus the actual land use pattern (Table 4), from which the overall accuracy and the Cohen's Kappa coefficient for all land use types were calculated. In addition, the agreement of the changes was validated using the figure of merit (Fom), which is superior to the Kappa coefficient in assessing the accuracy of simulated changes (Pontius & Millones, 2011; Pontius et al., 2008). This index can be expressed as the following equation:

Table 3
The neighborhood weights for individual land use type in different ecological regions.

Ecological regions	Cultivated land	Forest land	Grassland	Water area	Urban land	Unused land
The NASA region	0.5	0.1	0.2	0.1	1	0.3
The NSHS region	1	0.03	0.01	0.2	1	0.1
The SH region	0.2	0.01	0.3	0.4	1	0.5
The TP region	1	0.1	0.5	0.1	1	0.2

Note:.
NASA: the Northern Arid and Semi-Arid region.
NHSH: the Northeast Humid and Semi-Humid region.
SH: the Southern Humid region.
TP: the Tibetan Plateau region.

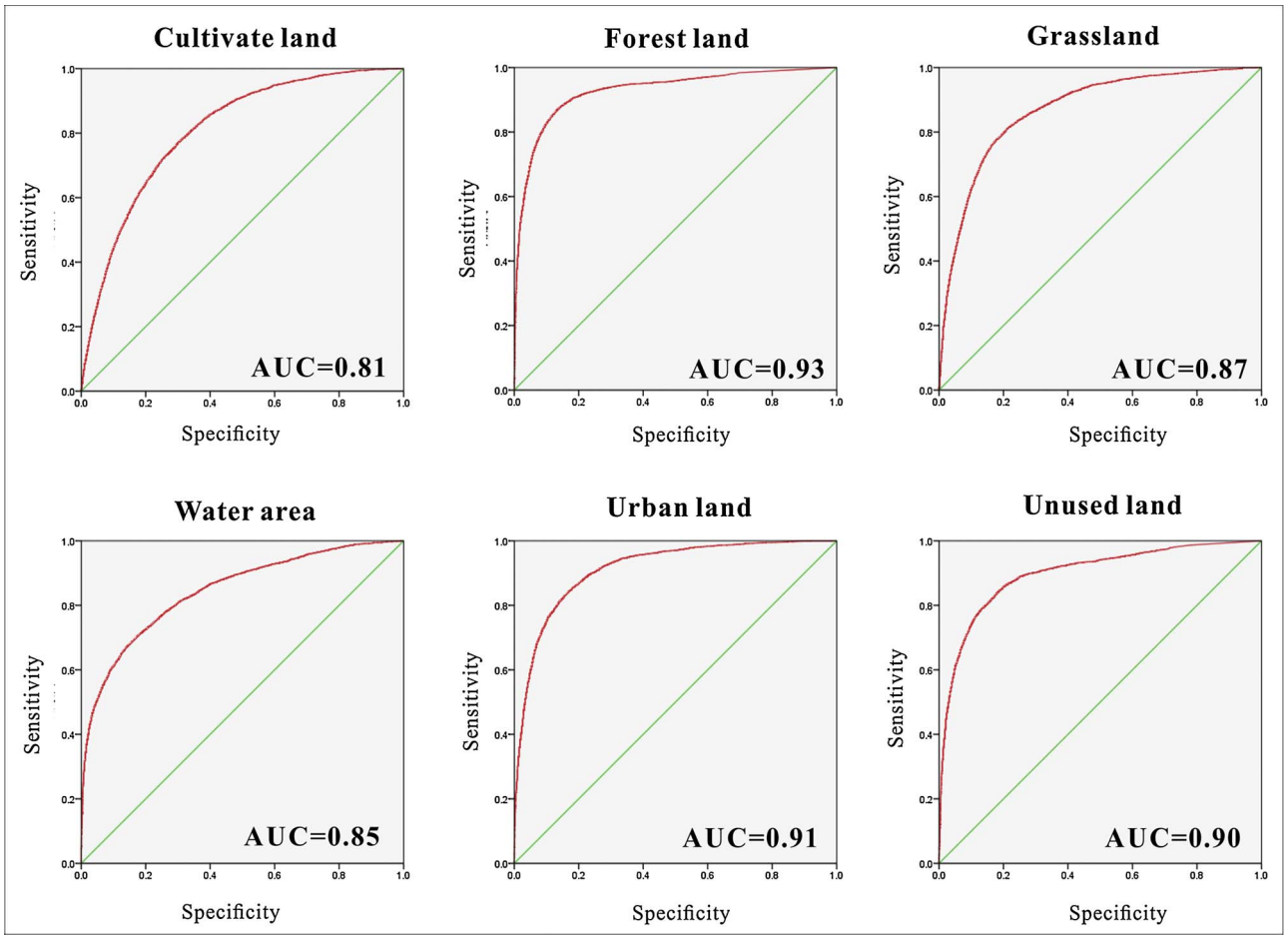

Fig. 8. ROC curves and AUC values of individual land use types fitted by the ANN.

$$\text{Fom} = \frac{B}{A + B + C + D} \tag{8}$$

where A is an area of error due to observed change predicted as persistence, B is an area of accuracy due to observed change predicted as change, C is an area of error due to observed change predicted as changing to an incorrect category, and D is an area of error due to observed persistence predicted as change.

For the accuracy assessment results, all three accuracy indexes are intermediate (the overall accuracy is 0.75, the Kappa coefficient is 0.67 and the Fom is 19.62%). Although a Fom value of 19.62% is not highly accurate, we believe it is acceptable for the Chinese region from 2000 to 2010 for the following reasons: 1) The Fom value of 19.62% has a similar range compared to the other simulation study results. For example, the Fom values range from 12% to 18% for the urban land-use dynamic modeling in the study by Chen, Li, Liu, and Ai (2014). Pontius et al. (2008) also reported a Fom range from 1% to 59% (most of the values are lower than 30%). 2) Pontius et al. (2008) reported a positive relationship between the Fom and observed net change. Due to this relationship, the Fom value of a long-period simulation result is most likely higher than one with a short period. (Estoque & Murayama, 2012a). In this article, our simulation period is relatively short (2000–2010), with a 17.38% observed net change, which is shorter compared to studies that have a relatively high Fom (Chen, Li, Liu, Ai, & Li, 2016; Estoque & Murayama, 2012b). Considering that our study area is a large region with complex climatic conditions and significant regional differences, the simulation accuracy is quite acceptable for the multiple land use simulations. The accuracy assessment indicates that the FLUS model is capable of tracing the spatial dynamics trajectories of multiple LUCCs in China with a relatively favorable accuracy.

To demonstrate the superiority of the proposed method over the existing multiple LUCC simulation models, we compared the performance of the proposed method to that of three well-accepted models: the Logistic-CA model (Li et al., 2013; Wu, 2002), the traditional ANN-CA model (Li & Yeh, 2002), and the CLUE-S model (Verburg et al., 2002). The Logistic-CA model predicts future land-use based solely on the neighboring land-uses and the same driving factors that are considered in the paper. The traditional ANN-CA model is typically applied to the simulation of multiple LUCCs via the integration of neural networks with cellular automata, but it does not consider the interaction and competition of different land use types. Moreover, the traditional CA model requires two sets of land use pattern data for fitting the transition probability from one land use type to another for the given driving factors, which inevitably introduces error propagation from the multiple land use classifications. Other simulation models use only one land use set to fit the probability-of-occurrence for specific land use types, such as the CLUE-S, DynaCLUE, CLUMondo and FORE-SCE models. The CLUE-S model selected in the comparison is a well-accepted multiple LUCC simulation model that uses empirically quantified relationships between land use and its driving factors in combination with dynamic modeling. However, the CLUE-S model estimates the probability-of-occurrence for each land use type separately, so it does not sufficiently address the competition among the different land use types.

In the comparative study, we applied the proposed FLUS model, the Logistic-CA model, the traditional ANN-CA model and the CLUE-S model to the Pearl River Delta (PRD) region of China to simulate the land use pattern from 2000 to 2010 at a spatial resolution of 250 × 250 m^2. For the FLUS method, we divided the study period into

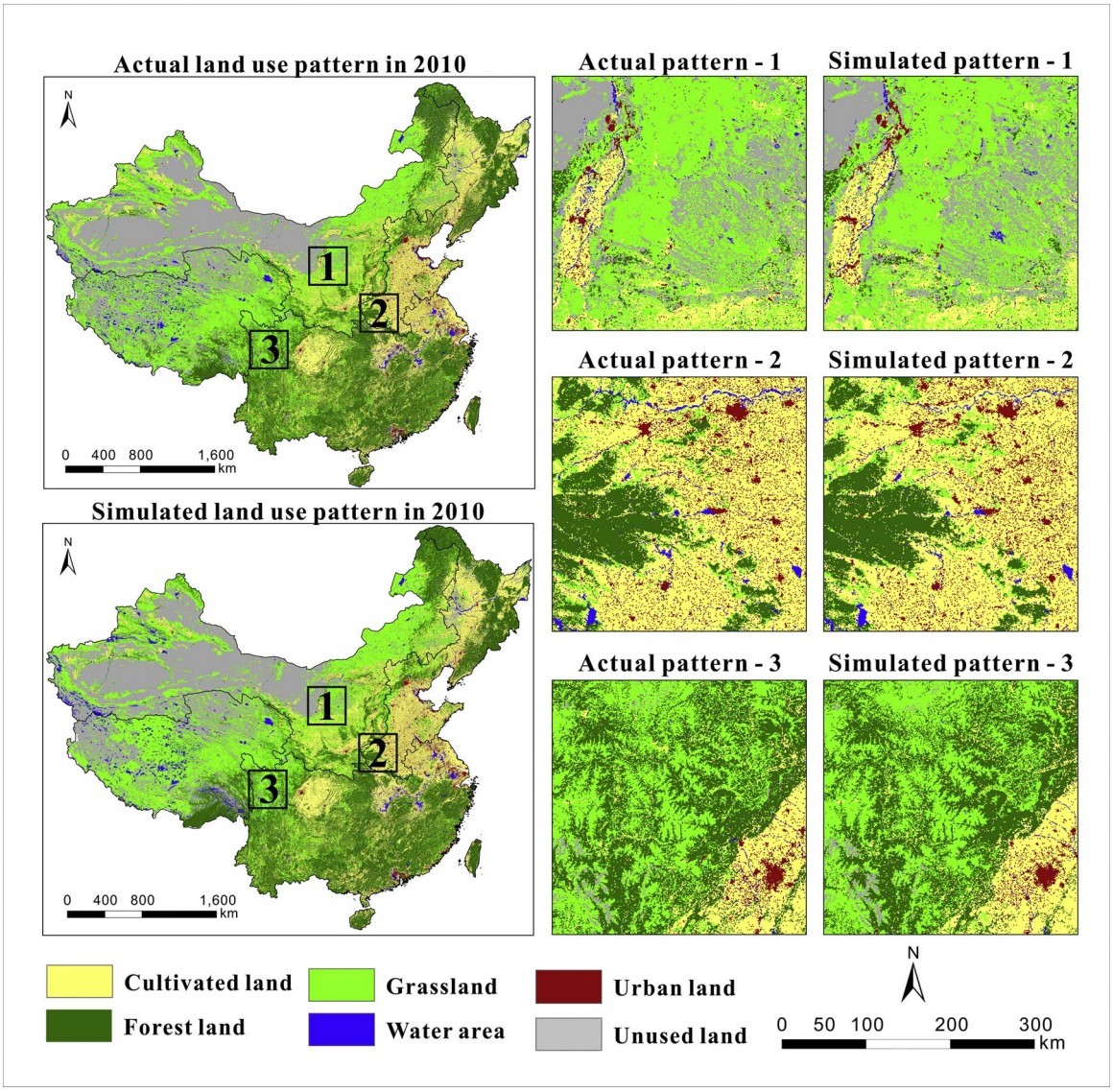

Fig. 9. The simulated land use pattern and the actual land use pattern in 2010.

two intervals, 2000–2005 and 2005–2010, during which the interactive coupling mechanism could be applied. An additional experiment in which the SD model was directly coupled to the CA model (2000–2010) was performed and compared to the proposed method to show the effectiveness of the interactive coupling mechanism.

The actual 2010 land use patterns and the simulation results of the five different methods are shown in Fig. 10. Even though all four models are capable of simulating multiple land use dynamics, the simulated patterns are slightly different from each other. Using urban land as an example, the ANN-CA model generates a relatively dispersed pattern compared to the actual observations, whereas the CLUE-S model tends to yield a relatively compact pattern. The pattern generated by the Logistic-CA model is more compact than that of the ANN-CA model but is more dispersed than the CLUE-S model pattern and contains additional urban enclaves. Both the direct coupling and interactive coupling FLUS models, however, were capable of simulating

Table 4
Confusion matrix of the predicted land use pattern versus the actual pattern in 2010.

Land use types	Actual land use in 2010						
	Cultivated land	Forest land	Grasslands	Water area	Urban land	Unused land	total
Cultivated land	101,521	15,891	8033	2656	7207	1060	136,368
Forest land	16,592	131,553	12,349	949	488	1472	163,403
Grasslands	8723	12421	65,814	737	402	7583	95,680
Water area	1670	579	903	7878	318	1542	12,890
Urban land	5698	1443	615	460	8826	84	17,126
Unused land	1765	993	7930	647	163	52,977	64,475
total	135,969	162,880	95,644	13,327	17,404	64,718	489,942

Kappa Coefficient = 0.67, Overall Accuracy = 0.75.

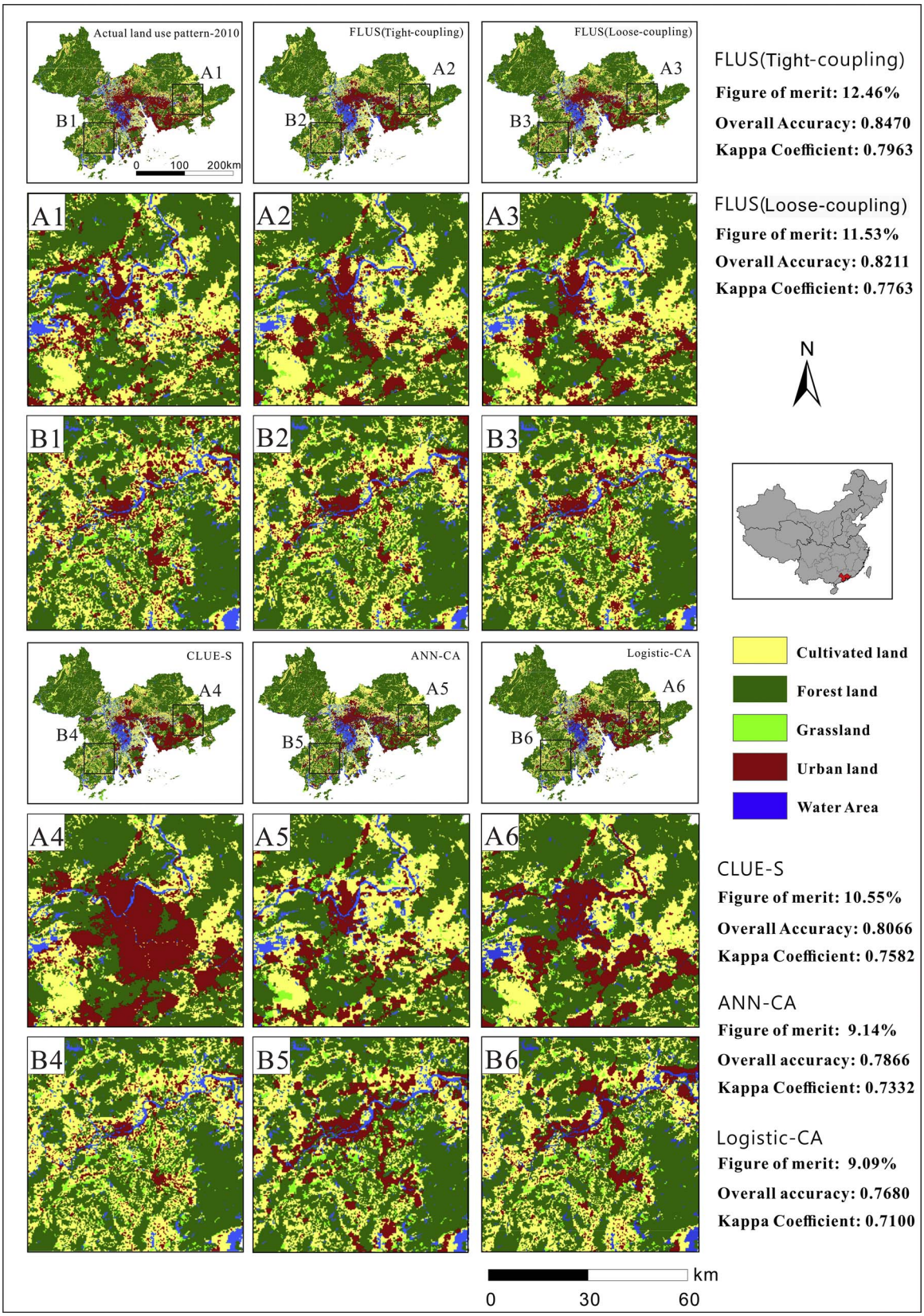

Fig. 10. Comparison of simulated land use pattern in the PRD region of China by using the Logistic-CA model, ANN-CA model, the CLUE-S model and the FLUS model (loose-coupling and tight-coupling).

more-realistic land use patterns that are neither too dispersed nor too compact. This favorable peculiarity is likely contributed by the proposed self-adaptive inertia and competition mechanism that was designed to address the complex local land use interactions and competitions. To quantitatively assess the overall performances of the four models, a total of 5000 samples were randomly selected across the PRD

Table 5
Rigid conversion cost of land use pairs for sensitivity analysis.

Land use types	Cultivated land	Forest land	Grass land	Water area	Urban land	Unused land
Cultivated land	0	0	0	0	0	0
Forest land	0	0	0	1	1	0
Grass land	0	0	0	0	0	0
Water area	0	0	0	0	1	0
Urban land	1	1	1	1	0	1
Unused land	0	1	0	0	0	0

region, from which the overall accuracy and the Cohen's Kappa coefficient were estimated. The Kappa coefficient only evaluates the overall consistency of the simulation results compared to the actual land use pattern and is unable to accurately incorporate information from recent changes. Therefore, we also used the Fom method to measure the accuracy of the land use changes in the comparison study. With the Fom statistics, the previously established land-uses (unchanged cell in 2000 land use) can be completely excluded from the validation, and the comparison between these models is entirely based on the recent change (land use change between 2000 and 2010).

The overall accuracy of the proposed method (~0.8470) is significantly higher than that of the CLUE-S model (~0.8092), the ANN-CA model (~0.7866), and the Logistic-CA model (~0.7680). Similarly, the Kappa coefficient of the proposed method (~0.7963) is better than that of the CLUE-S model (~0.7682), the ANN-CA model (~0.7332), and the Logistic-CA model (~0.7100). Moreover, the 'Figure of merit' (Fom) indicator was calculated to evaluate the land use change accuracy. For the FLUS model results, the Fom value is 12.46%, which is higher than the values of the other models (ranging from 9.09% to 10.55%).

3.2.3. Examining the integration of SD and CA

A comparison between the simulation results of FLUS (Tight-coupling) and FLUS (Loose-coupling) indicates that the former yielded a slightly better overall accuracy (0.8470 versus 0.8211), Kappa coefficient (0.7963 versus 0.7863) and Fom statistics (12.46% versus 11.53%) compared to the loose-coupling FLUS model. These comparisons showed that the proposed FLUS model performs better than the existing models for multiple land use dynamic simulations, and the integration between SD and CA yields a better simulation result with higher simulation accuracy. Although the improvement is not very significant, it does illustrate the effectiveness of the integration mechanism.

3.3. Model sensitivity to conversion cost

The conversion cost in this article is similar to the transition matrix used by many other models (Schaldach et al., 2011; Verburg et al., 2002); however, it acts as an extension and is more detailed than the conventional transition matrix. Here, we examine the model sensitivity to the conversion cost in the Pearl River Delta (PRD) region of China. We compare the model performance of three simulation results that separately apply 1) a conversion cost that allows all conversions, 2) a rigid conversion cost (see Table 5) and 3) a flexible conversion cost to the FLUS model simulation (see Table 1).

For a conversion cost that allows all conversions, all values are assumed to be 0, which indicates that all land use pair conversions are possible and at zero cost. The rigid conversion cost shown in Table 5 has been widely used by many other studies (Schaldach et al., 2011; Verburg & Overmars, 2009), but it only defines whether a conversion between one land use type and another is possible. A value of 1 denotes that a conversion is not allowed, and a value of 0 denotes that a conversion is possible in a rigid conversion cost matrix. The flexible conversion cost used in this article is defined based on the rigid conversion

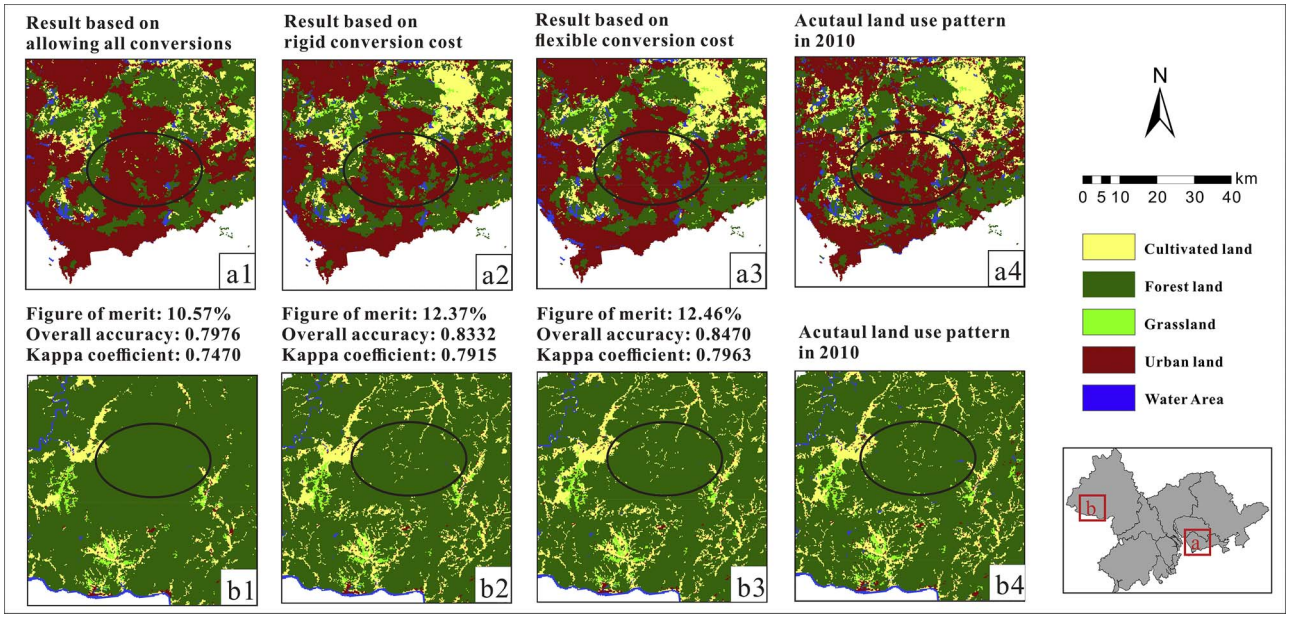

Fig. 11. Sensitivity analysis: region a, b are example areas to zoom in on. (a1), (b1): Land use map generated by allowing all conversions; (a2), (b2): Land use map generated by using rigid conversion cost; (a3), (b3): Land use map generated by using flexible conversion cost; and (a4), (b4): Actual land use pattern in 2010.

cost, which has been described in detail in Section 2.

When allowing all land use pair conversions, the results of the Fom value, the overall accuracy and the Kappa coefficient were 10.57%, 0.7976, and 0.7470, respectively. All of the accuracy indexes are higher than the results projected by the ANN-CA model (Fom = 9.14%, Overall accuracy = 0.7866, and Kappa coefficient = 0.7332) and the Logistic-CA model (Fom = 9.09%, Overall accuracy = 0.7680, and Kappa coefficient = 0.7100) but are slightly lower than the CLUE-S model for the overall accuracy and Kappa coefficient (Fom = 10.55%, Overall accuracy = 0.8066, and Kappa coefficient = 0.7582). Under such circumstances, the isolated cultivated patches surrounded by forest and the forest parcels circled by urban areas can more easily be converted to other land uses in this pattern (example in Fig. 11a1, b1). This phenomenon can be suppressed, and a higher-accuracy simulation pattern can be generated by using a rigid conversion cost (Fom = 12.37%, Overall accuracy = 0.8332, and Kappa coefficient = 0.7915). Fig. 11 also shows that the distinctions between the other two simulation patterns are insignificant, but all the accuracy indexes are improved by using a flexible conversion cost (Fig. 11,a3, b3) instead of the rigid conversion costs (Fig. 11, a2, b2). The Fom value is improved to 12.46%, the overall accuracy is increased to 0.8470, and the Kappa coefficient is increased to 0.7963.

The sensitivity analysis indicates that the simulation results of the FLUS model are not very sensitive to the flexible conversion cost variations if the rigid conversion cost has been properly set; however, appropriate conversion cost values improve the simulation accuracy. Notably, an inappropriate rigid conversion cost can have relatively large negative effects on the model performance. Hence, the FLUS model still relies on expert judgment and model calibrations.

4. Scenario simulation of future LUCC in China for 2010–2050

4.1. Scenario description and parameterization

Before simulating the future land use dynamics, the demands for each land use type should be projected. By using the SD model, we investigated the influence of multiple driving force variables (economic development, population growth, technological innovation and climate change) on land use demands in different scenarios from 2010 to 2050. Four scenarios are designed based on the IPCC assessment reports (Sohl et al., 2012) while considering regional climate variations together with different socio-economic developments in China. As shown in Fig. 12, four scenarios are designed and organized along two axes, with the vertical axis representing human influence and the horizontal axis representing the natural environment. Each scenario is characterized by a range of alternative future conditions regarding human influence and the natural environment.

The baseline development scenario (BD_Scenario) is constructed based on the trajectory of past and current development in China. The current trends for economic and population development and technological innovation are assumed to remain continually consistent. Moreover, the climate is assumed to maintain its current temperature and precipitation rates (B1 climate scenario in the IPCC report). The fast development scenario (FD_Scenario) is designed to maximize the socio-economic benefits in China. The economy and population increase at a high speed, and science and technology develop rapidly. Additionally, intense climate change occurs in this scenario with sharp temperature and precipitation increases due to massive human activities accelerating greenhouse gas emissions and exacerbating

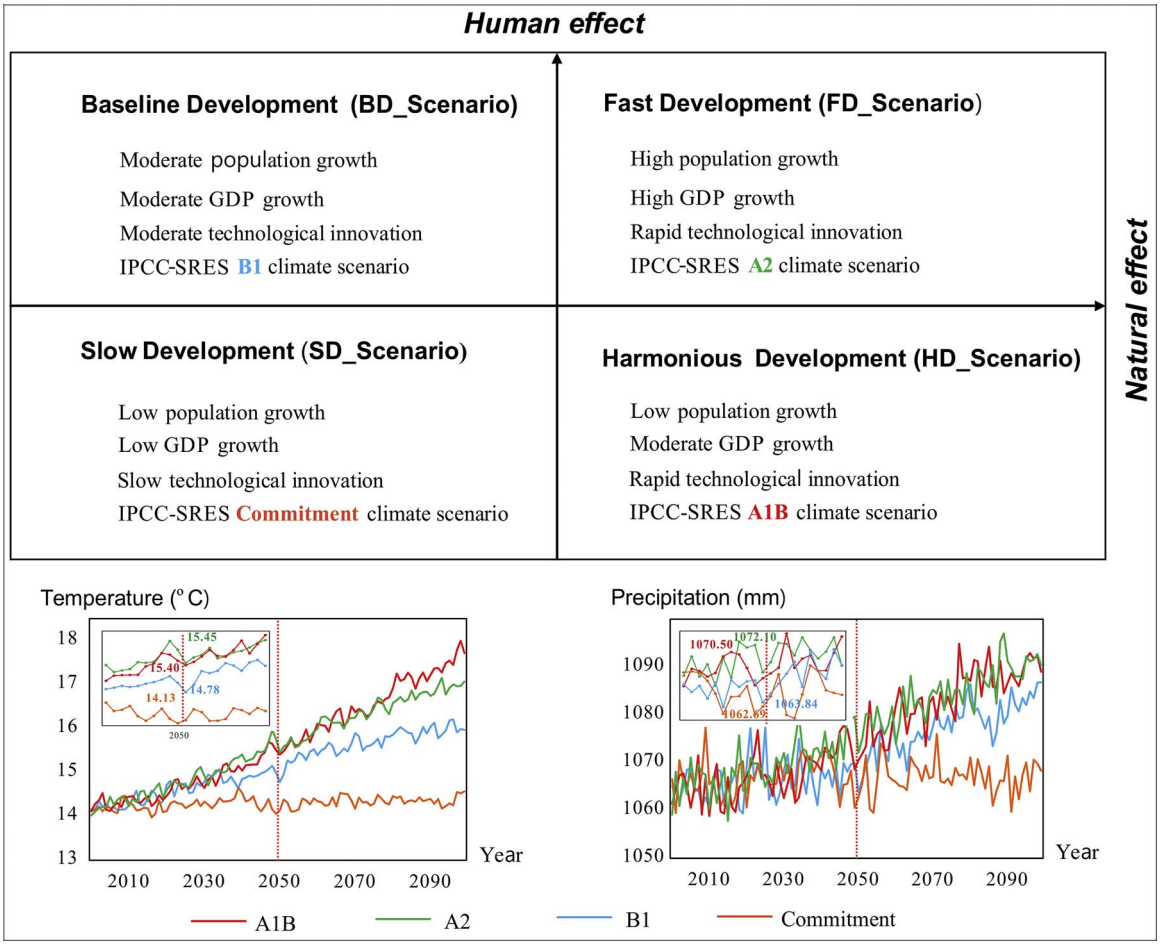

Fig. 12. Configurations of four development scenarios with regard to human and natural effects.

precipitation heterogeneity (A2 climate scenario in the IPCC report). Contrary to the FD_Scenario, the slow development scenario (SD_Scenario) is constructed to predict the land use demands under the influence of slow socio-economic growth and moderate climate change. The GDP growth rate, population growth rate, and technological innovations are assumed to be at the lowest levels in this scenario. In addition, the scenario is assumed to rarely experience extreme weather events and has slow annual temperature and precipitation changes (commitment climate scenario in the IPCC report). Lastly, the harmonious development scenario (HD_Scenario) is a more human-oriented and sustainable development mode. Steady population growth and moderate development-oriented economic growth are considered in this scenario, and the proportion of technological investments is assumed to have more input in agricultural productivity. Moreover, the natural environment will change moderately (A1B climate scenario in the IPCC report), which is assumed to have a positive impact on land use changes in this scenario.

To parameterize these scenarios into the SD model for projecting the future land use demands, five parameters, including both socio-economic and natural influences, are considered in different scenarios: annual population growth (APG), annual economic growth (AEG), annual technological innovation (ATI), annual temperature change (ATC) and annual precipitation change (APC). Moreover, these parameters are set to be slightly different in the four regions to reflect the social and ecological differences among these regions. The parameterization details for each scenario in the different regions are shown in Table 6.

As a potential developed country, China has become the fastest-growing economy worldwide over the past two decades. Although the economic growth has slowed in recent years (actual GDP growth fell from 10.4% in 2010 to 7.8% in 2012 to 6.9% in 2015), China is attempting to maintain its annual GDP growth at ~6.5% in the near future, according to China's thirteenth Five Year Plan. Therefore, the Chinese economy is undoubtedly going to continue to rise. However, the growth rate is unclear because the Chinese economic policies will introduce much uncertainty. In this study, four different economic development trajectories were designed for the different scenarios with different annual GDP growth rates over the next 40 years. Closely linked to the economic growth, the population growth is another important driving force for land use changes. We established four population growth modes that approximately correspond to the economic trend for each scenario. Technological development is also considered an important driving factor in the scenario simulations because technological development not only improves agricultural productivity but also reduces the land resource consumption necessary to support human welfare. Based on the current technological development in China, we assumed different future cases of technological innovation for the next 40 years in each scenario. Considering the regional differences in economic development and population growth, the annual GDP and population growth are set to be slightly different in the four sub regions according to historical socio-economic statistical data. The BD_Scenario tends to follow a moderate trend for economic and population development, e.g., the APG (~0.6%) and AEG (~7%) maintain the current growth levels. The technological investment in agricultural productivity is set to a 10% annual growth rate to be consistent with the current state. In the FD_Scenario, the population growth and economic growth are assumed to experience sustained and rapid increases (~0.9% and 8%, respectively) at the expense of many natural resources. A 15% growth rate is set for the agricultural productivity ATI to support the large population expansion and rapid economic development. In contrast to the FD_Scenario, the SD_Scenario has a relatively slow growth rate for both the population (~0.5%) and the economy (~5%), as it is designed to simulate the LUCC under conservative and environmentally friendly development. A relatively low ATI (5%) is considered in this scenario. The HD_Scenario is a more idealistic and sustainable development strategy that maintains a steady and intermediate AEG (~7%) while protecting the natural environment with appropriate policies. The population in this scenario is assumed to have a relatively slow growth rate (0.5%) to reduce the impact on the natural environment. The ATI growth rate is set to be the highest (20%) among all the scenarios.

Table 6
Parameterization of the socio-economic and natural factors in the four designed scenarios.

Scenarios	Factors	NASA region	NSHS region	SH region	TP region
Baseline development scenario (BD)	APG (%/a)	0.65	0.53	0.62	0.91
	AEG (%/a)	6.50	6.80	7.00	8.50
	ATI(%/a)	10	10	10	10
	APC (mm/a)	0.5721	0.8390	0.4770	2.9480
	ATC (°C/a)	0.0361	0.0314	0.0452	0.0451
–					
Fast development scenario (FD)	APG (%/a)	0.95	0.67	0.76	1.40
	AEG (%/a)	7.50	7.70	7.97	10.03
	ATI(%/a)	15	15	15	15
	APC (mm/a)	0.8358	1.2259	0.6970	4.3072
	ATC (°C/a)	0.0651	0.0567	0.0817	0.0681
Slow development scenario (SD)	APG (%/a)	0.50	0.34	0.47	0.85
	AEG (%/a)	5.50	4.90	5.20	7.24
	ATI(%/a)	5	5	5	5
	APC (mm/a)	0.0226	0.0331	0.0188	0.1162
	ATC (°C/a)	0.0035	0.0030	0.0044	0.0044
Harmonious development scenario (HD)	APG (%/a)	0.55	0.47	0.47	0.80
	AEG (%/a)	6.80	7.00	6.91	8.12
	ATI(%/a)	20	20	20	20
	APC(mm/a)	0.7910	1.1601	0.6596	4.0761
	ATC (°C/a)	0.0544	0.0474	0.0683	0.0681

Note:.
APG: Annual Precipitation Growth.
AEG: Annual Economic Growth.
ATI: Annual Technological Innovation.
APC: Annual Precipitation Change.
ATC: Annual Temperature Change.

4.2. Land use demand projection

According to the four different scenarios described in the previous section, the system dynamics model was used to project the land use demands in the four sub-regions of mainland China under different development scenarios. A summary of the land use demands in each scenario over the next 40 years is shown in Fig. 13. As expected, the urban land area will increase consistently from 2010 to 2050 for all scenarios due to the population increase. In the FD_Scenario, the urban land has a dramatic growth to ~400 thousand km^2 by 2050, almost twice that in 2010. The rapid expansion of urban land in this scenario is likely due to the fast urbanization process, which requires an increase in developed areas to accommodate the population and economic growth. Conversely, the lowest increase in urban land is associated with the SD_Scenario, which is designed to represent the conservative and environmentally friendly development scenario. In the BD_Scenario and HD_Scenario, urban land moderately increases compared to the SD_Scenario and FD_Scenario. Unlike the urban land demands, the cultivated land variation tendencies are quite different among the four designed scenarios. In the SD_Scenario and HD_Scenario, cultivated land tends to decrease because human activities are likely to occupy cultivated land around the cities and convert it into urban land. However, the population pressure in the FD_Scenario and BD_Scenario will cause an increase in food production demand and result in an increase in cultivated land. The projected forest land will decline in the BD_Scenario, FD_Scenario and the SD_Scenario. However, it will increase to a total area of 2.5 million km^2 in the HD_Scenario in 2050. The grassland area moderately increases in the HD_Scenario but remains relatively stable in the other three scenarios over the next 40 years.

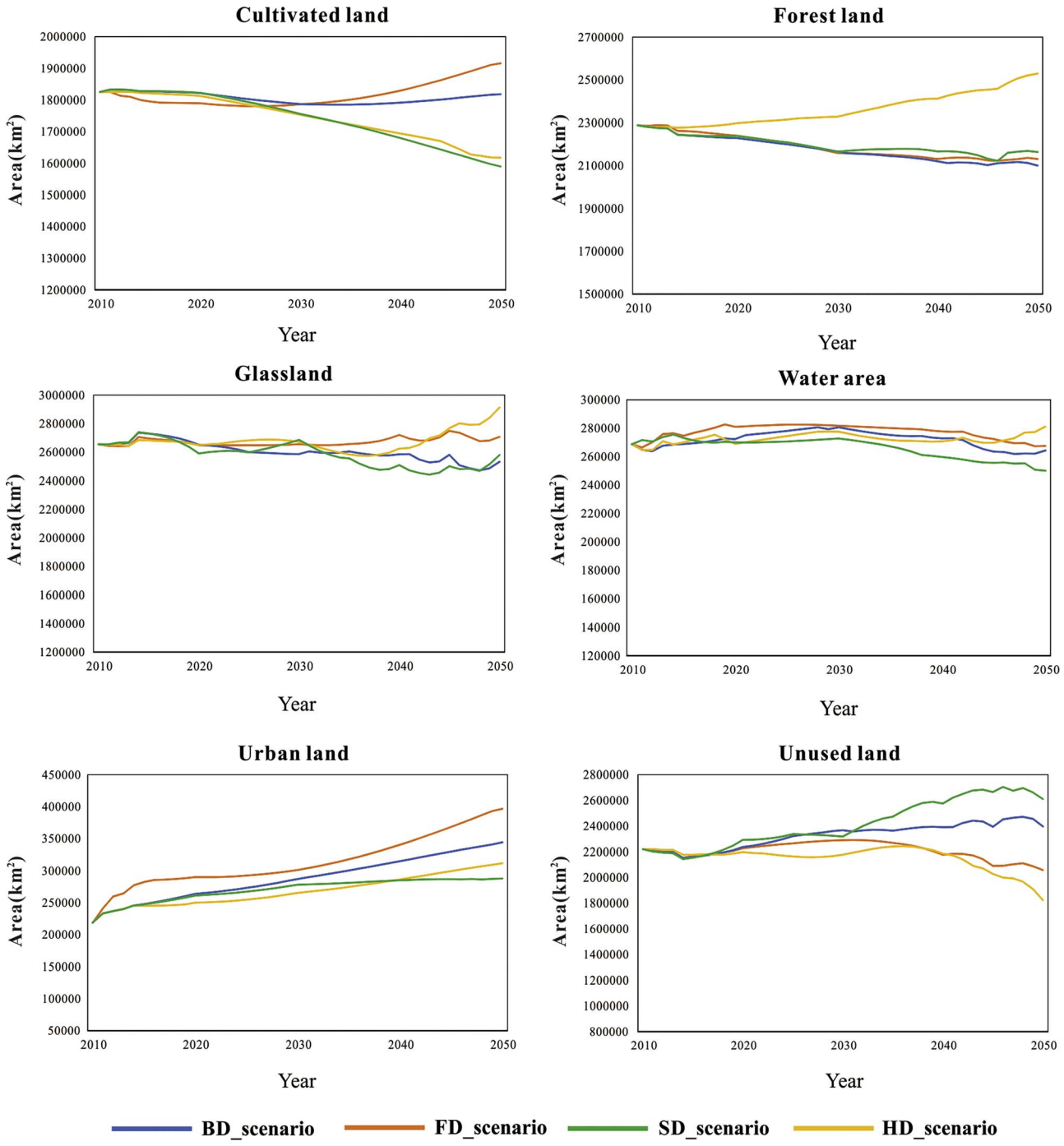

Fig. 13. Projection of land use demands under different scenarios in mainland China from 2010 to 2050.

These forest and grassland increases in the HD_Scenario are likely attributable to the trade-off between the ecological and socio-economic benefits. In the SD_Scenario, a large amount of grassland, forest and water will be converted into the unused land (e.g., sandy land, Gobi, salina, swampland, bare soil, bare rock, alpine desert and tundra). In the HD_Scenario and the FD_Scenario, however, the unused land tends to decrease after 2030, indicating that the unused land is used for development purposes in these two scenarios.

4.3. Spatial simulation and analysis

Based on the multiple land use demands projected in the previous section, we used the multiple CA model to simulate the spatial LUCC dynamics in the four designed scenarios from 2010 to 2050. The simulation results of the BD_Scenario, FD_Scenario, SD_Scenario and HD_Scenario in 2050 are shown in Fig. 14. The figure shows that the proposed multiple CA model can predict the spatial pattern of multiple land use types in 2050. Compared to the actual land use pattern in 2010, we found that the urban land expansion in all scenarios is primarily located around current metropolitan areas and in the eastern coastal regions. Most of the grassland is distributed in the eastern Qinghai-Tibetan Plateau and northern Inner Mongolia, while the cultivated lands are predominantly located in the Sichuan Basin and in the plains, such as the North China Plain, Sanjiang Plain and Songnen Plain in the Heilongjiang Province. The forest is primarily concentrated in the southern low hilly areas and the northeast mountainous areas in China.

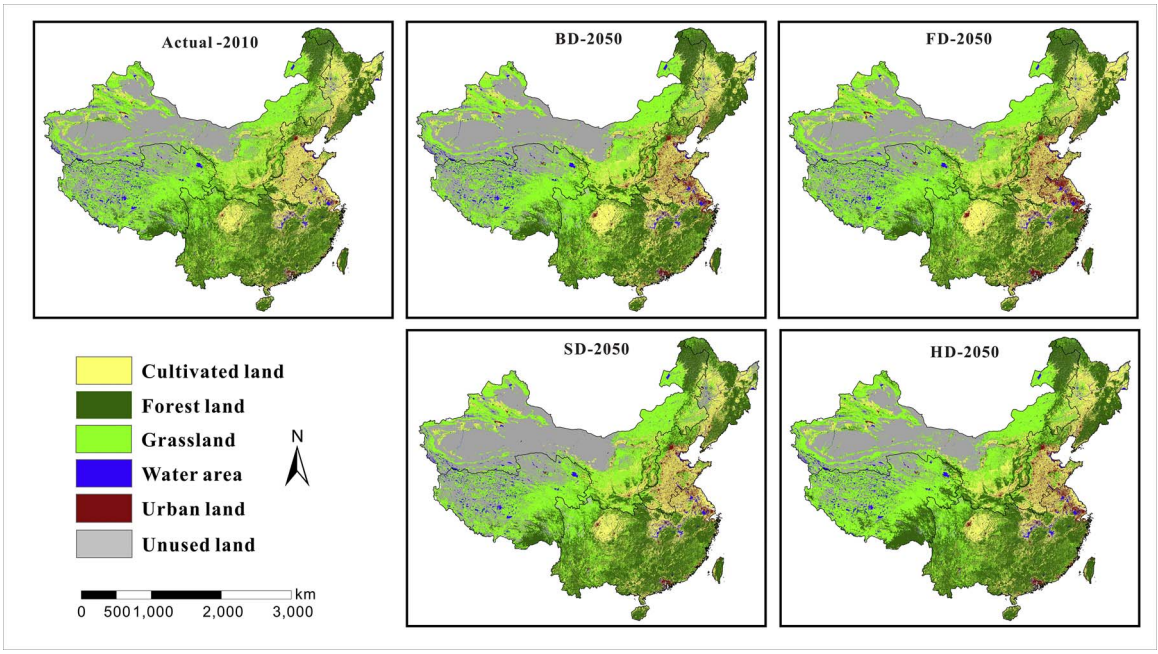

Fig. 14. Simulated spatial pattern of land cover in the four designed scenarios from 2010 to 2050.

In addition, central northwestern China remains as unused land, including a large area of the Gobi Desert, bare soil, and alpine desert. To better highlight the spatial variability among the different scenarios, the percent change for each land use type at the local administrative level is calculated and shown in Fig. 15.

The spatial details of multiple LUCCs among the different scenarios can be examined at a regional scale. We focus on three enlarged regions that are representative of the changes in different land use types in individual scenarios. The first region, located in the NHSH sub-region, is selected to illustrate the different cultivated land distributions among the four scenarios (Fig. 16). As shown in the figure, the land surface of this region is primarily covered by cultivated land, with a number of forest patches in the east and grasslands scattered in the west. Compared to the actual land use pattern in 2010, the most significant LUCC in the BD_Scenario involves the large-scale abandonment of cultivated land in the southwest corner, converted to grassland or unused land, likely due to soil degradation after excessive reclamation. This scenario is much more severe in the SD_Scenario due to the conservative development strategy. In contrast, much unused land converts to grassland and cultivated land by 2050 in the FD_Scenario. This may be due to the more adequate rainfall and proper reclamation in the two scenarios. Since FD_Scenario is marked by rapid population growth and a fast-growing economy, unused land reclamation is necessary to meet the large food production demand, leading to the wide expansion of cultivated land and grassland in this scenario. Compared to the economy-oriented FD_Scenario, the HD_Scenario is characterized by sustainable development. It describes a future land use pattern in which grassland restoration occurs on unused lands as efforts are made to preserve biodiversity and to improve the ecosystem quality.

Fig. 17 shows the second enlarged region in the Yangtze River Delta, which is characterized by typical urban land development and expansion under different human and natural impacts. In the economic-oriented FD_Scenario, a dramatic expansion of urban land and a corresponding decrease in cultivated land around major metropolitan areas occurs over the next 40 years. The same occurs at a slightly slower rate in the BD_Scenario. The rapid expansion of urban areas in these two scenarios likely results from the demand for infrastructure construction for socio-economic development and significant population increases. In contrast, the SD_Scenario has the smallest urban expansion by the end of 2050 due to lower population pressures and economic growth during the study period. The HD_Scenario maintains a similar grassland and forest land pattern compared to the SD_Scenario, even though the influences of human activities and the natural environment are different between these two scenarios. In addition, a reasonable amount of urban land expansion occurs, which relieves the pressure of the increasing demand from socio-economic development. Moreover, China's largest freshwater lake (Poyang lake), located in the southwestern corner of the region, may experience a significant water area restoration in the HD_Scenario compared to the others. This is due to the combined effects of a precipitation increase and a series of environmental protection acts for this scenario.

Fig. 18 shows another region located on the border between the Qinghai and Gansu provinces that illustrates the land use changes in a farming-pastoral ecotone in an ecologically sensitive region. Compared to the land use pattern in the baseline year of 2010, both forest and grasslands in this region experience significant changes in the four scenarios. The most significant change is the extensive expansion of forest and grassland in the HD_Scenario. This phenomenon is likely related to the humid climate conditions that provide sufficient water for vegetation growth and the environmental development strategy in this scenario. The grassland in the FD_Scenario slightly decreases and is converted to cultivated land, likely due to the influences of rapid population and economic growth. In contrast, the forest cover will experience a modest reduction in the BD_Scenario, although forest tends to experience density increases in some places. Another significant change in the SD_Scenario is that the forest land sharply declines throughout the entire region and is converted to grassland. Moreover, the grassland in the northeast corner decreases significantly and becomes unused land due to the lack of precipitation in the SD_Scenario. These results show that land use changes more prominently in an ecologically sensitive region.

5. Discussion

In this study, we discussed the FLUS model performance with the 1000-m spatial data in China from 2010 to 2050. The simulated 2010 land use pattern was compared to the actual land use pattern to measure the model performance. The overall accuracy of the simulated land use pattern is 0.75 for all land use types, the Cohen's Kappa coefficient is 0.67, and the Fom value is 19.62%. Moreover, we compared the

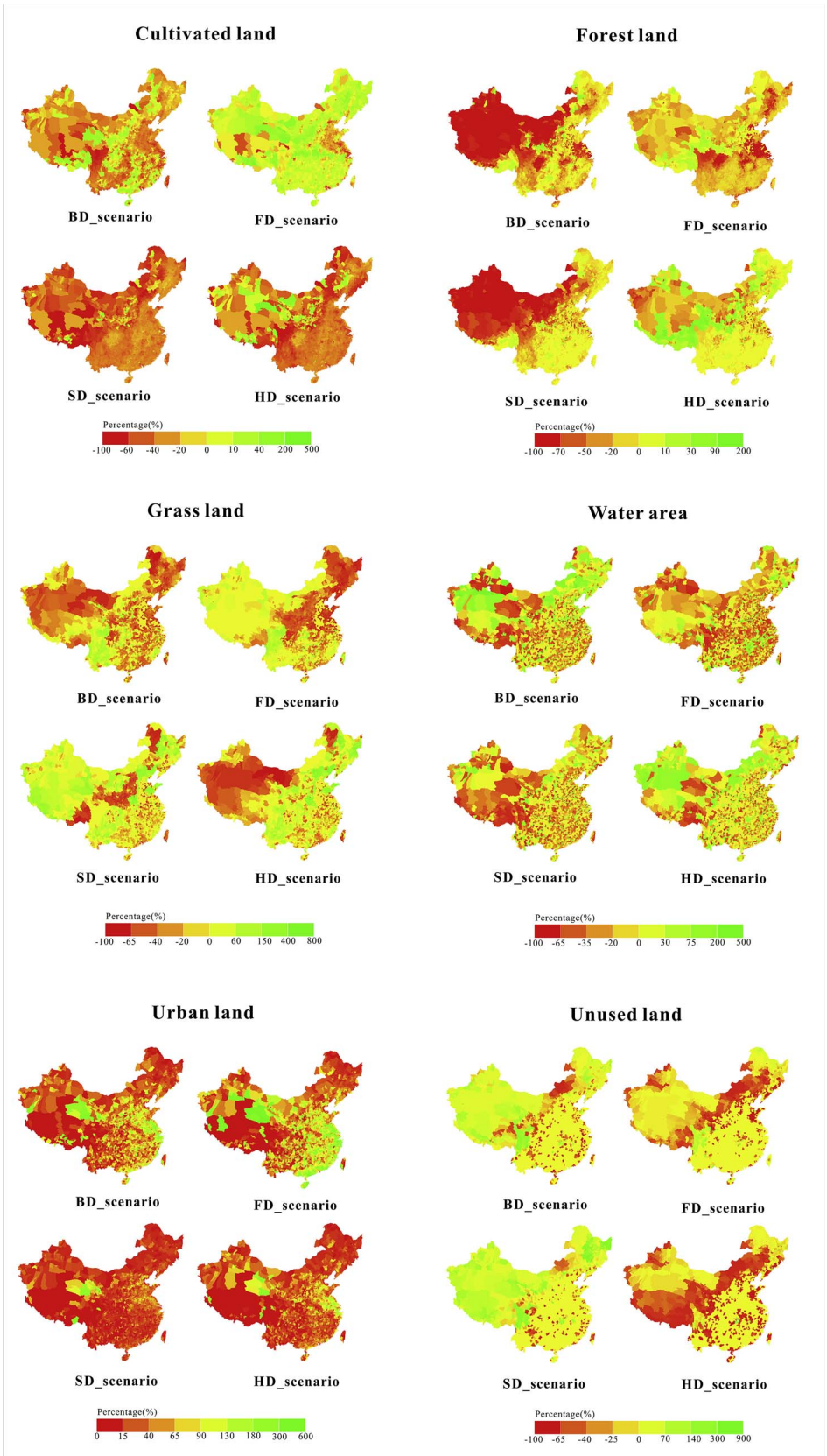

Fig. 15. Land cover change percentage at local administrative level in different scenarios.

proposed method to the well-accepted Logistic-CA, CLUE-S and ANN-CA models by applying these three models to the Pearl River Delta (PRD) region in China for the land use simulation in 2010. The comparison shows that the proposed method can simulate the land use dynamics in a more realistic manner due to the use of the self-adaptive inertia and competition mechanism. This mechanism allows the model to process complex local land use interactions and competition. Moreover, the improvement is attributed to the interactive coupling

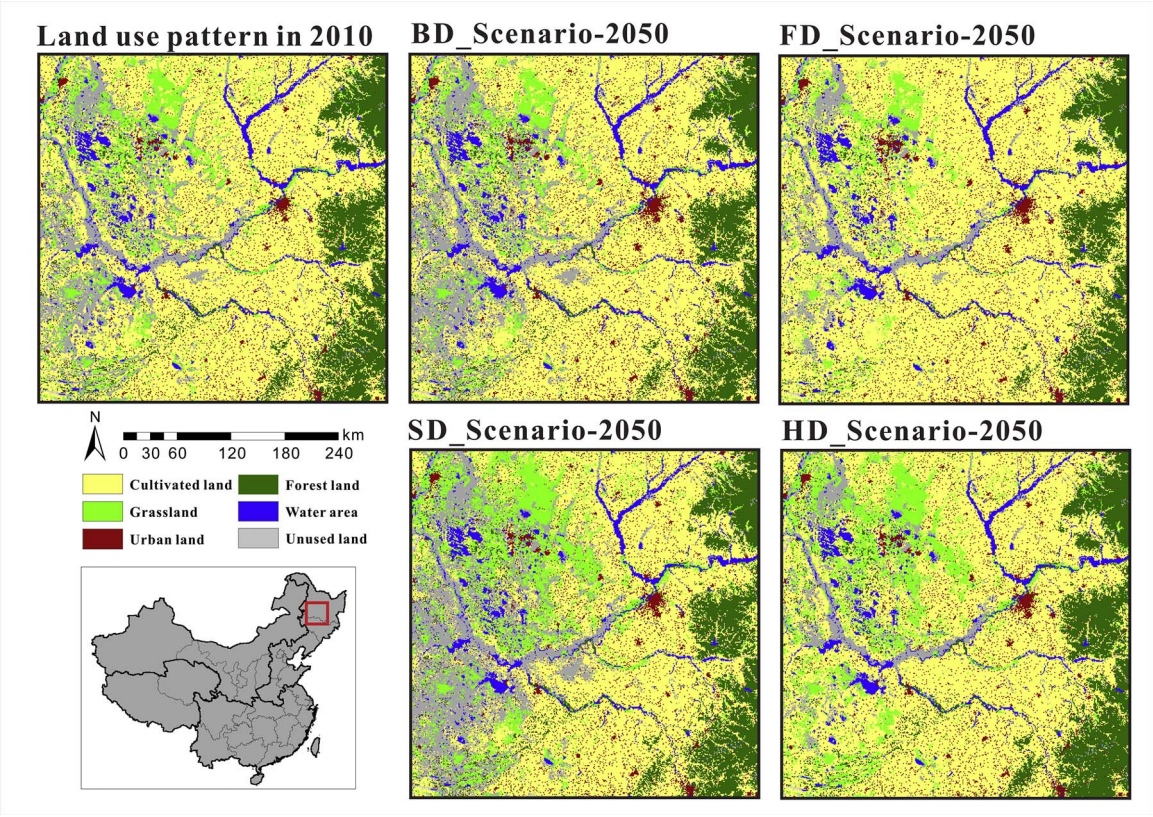

Fig. 16. Simulation of typical cultivated land patterns in different scenarios by 2050.

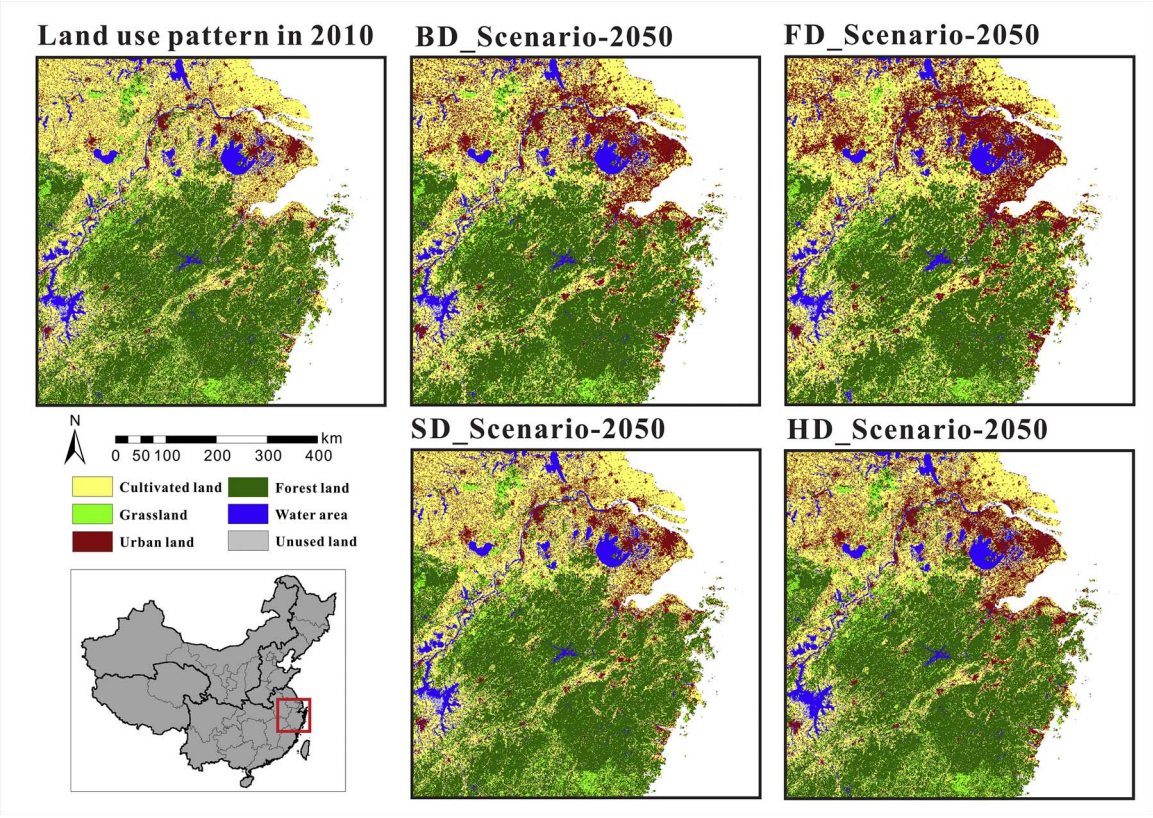

Fig. 17. Simulation of typical urban land patterns in different scenarios by 2050.

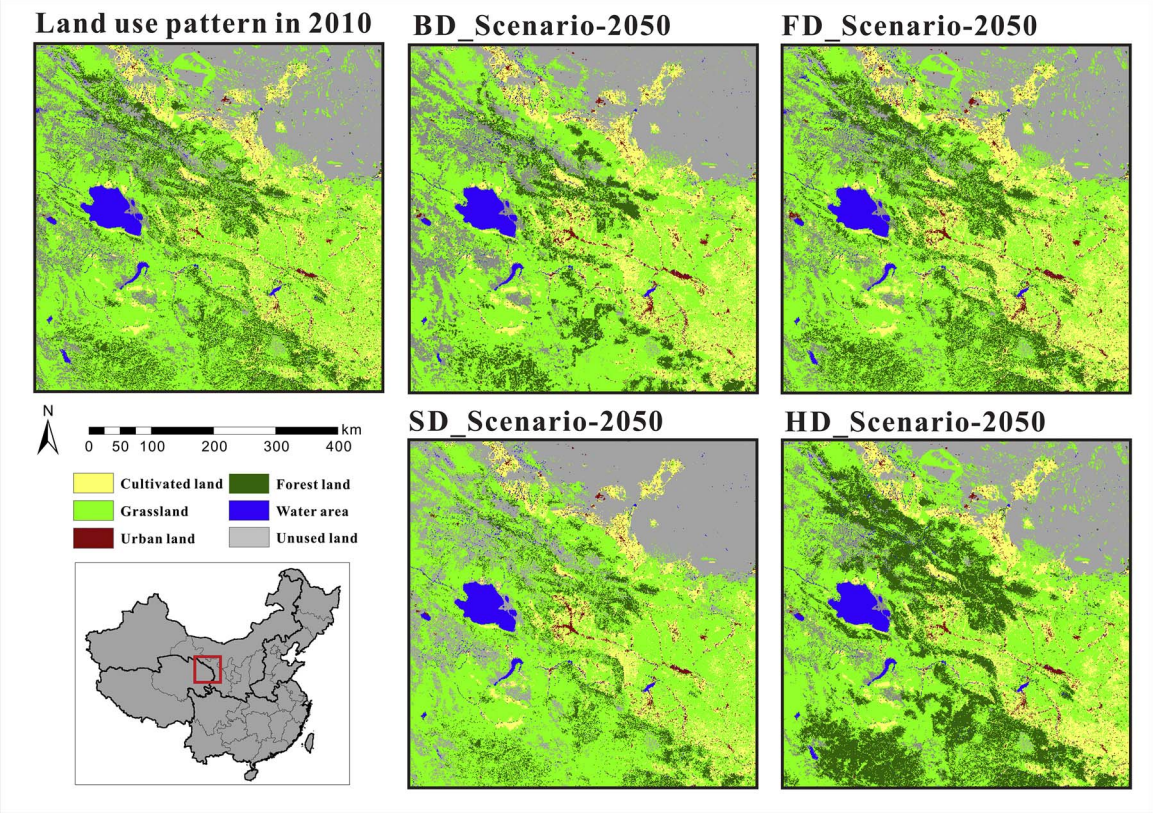

Fig. 18. Simulation of typical farming-pastoral ecotones in different scenarios by 2050.

mechanism, which enables the SD and CA models to evolve collaboratively according to the comparison of tightly coupled and loosely coupled FLUS models. The sensitivity analysis indicates that the model is insensitive to the conversion cost variation if the conversion cost values are approximately correlated with the actual regional costs.

Four scenarios in 2050 depicting different development strategies were designed to consider socio-economic developments (population, GDP, and technological innovation) and natural climate changes (temperature and precipitation). Based on the designed scenarios, we simulated the future land use dynamics of these scenarios, namely, the baseline development scenario (BD_Scenario), the fast development scenario (FD_Scenario), the slow development scenario (SD_Scenario) and the harmonious development scenario (HD_Scenario), by using the proposed FLUS method. The analysis of these simulated land use patterns yields the following conclusions: 1) Urban land tends to expand in all scenarios, especially in the fast development scenario (FD_Scenario), followed by the baseline development scenario (BD_Scenario). Urban expansion primarily occurs in the eastern coastal area. 2) Cultivated land significantly increases in the fast development scenario (FD_Scenario) and baseline development scenario (BD_Scenario) due to the population pressure. However, in the harmonious development scenario (HD_Scenario), cultivated land tends to decrease despite a slight increase in the population, subject to the technological improvements. 3) In ecologically sensitive regions, the forest and grassland areas will significantly decline if they are not well protected. Grassland and cultivated land will likely be converted into unused land due to over-reclamation and a low precipitation rate.

In a future study, we will test the model's applicability for higher-resolution simulations. Another limitation associated with this model is that patch developments cannot be simulated, thus causing simulation biases. We will improve this in the future by adding a patch development mechanism (Chen et al., 2016) to the FLUS model. Moreover, the FLUS model transition rules (referring primarily to the conversion cost and the well-trained ANN model) are assumed to be unchanged during the simulation process, while these rules may change over a long period (e.g., 50 or 100 years) in the real world. We will invest more effort in tackling this challenge in future works.

6. Conclusions

Land use simulation models are effective and reproducible tools to analyze both the causes and consequences of alternative future landscape dynamics relative to socio-economic and natural environmental driving forces. Complex linkage and feedback structures need to be understood to simulate multiple land use conversions under uncertain future conditions. In this paper, we present an approach that integrates top-down system dynamics (SD) with bottom-up cellular automata (CA) for the simulation of multiple LUCC dynamics. To address the natural environmental effects, we propose a solution for simulating the spatial trajectories of multiple LUCCs under human-nature-included scenarios. The top-down SD model is used to represent the major impacts of socio-economic and climatic changes on land use demands. A self-adaptive inertia and competition mechanism is incorporated within the CA model to process the complex competitions and interactions among the different land use types. The top-down SD demand projection model and the bottom-up CA local allocation model are interactively coupled during the simulation.

The proposed model was applied to the LUCC simulations in China from 2000 to 2010 to test the model's applicability and compare it with other studies. The FLUS model obtained the highest simulation accuracy and generated a more realistic land use pattern. The simulation results in mainland China driven by four future scenarios demonstrate that the FLUS model can be effectively used to identify hot-spot areas and analyze both the causes and consequences of future land use dynamics, which can help researchers and decision makers draft appropriate policies to better adapt to the rapid change of the natural environment under the background of global climate warming.

In summary, the proposed model is applicable for exploring the

impacts of climate change and human activities on future land use dynamics. The future land use developments in China will need to endure the effects from both climate change and economic/population growth. Effective measures should be used to address these effects to sustainably develop China in the future. Therefore, this study shows that the GeoSOS-FLUS software (available for download at http://www.geosimulation.cn/flus.html) can conveniently explore the possible patterns of multiple land use changes under the influence of both human and natural effects.

Acknowledgments

This research was funded by the National Key R & D Program of China (No. 2017YFA0604402 and 2017YFA0604404), the Key National Natural Science Foundation of China (Grant No. 41531176), and the National Natural Science Foundation of China (Grant No. 41671398).

References

Aerts, J. C., & Heuvelink, G. B. (2002). Using simulated annealing for resource allocation. *International Journal of Geographical Information Science, 16*, 571–587.
Bakker, M. M., Govers, G., Kosmas, C., Vanacker, V., Oost, K. V., & Rounsevell, M. (2005). Soil erosion as a driver of land-use change. *Agriculture Ecosystems & Environment, 105*, 467–481.
Batty, M., Couclelis, H., & Eichen, M. (1997). Urban systems as cellular automata. *Environment and Planning B: Planning and Design, 24*, 159–164.
Berling-Wolff, S., & Wu, J. (2004). Modeling urban landscape dynamics: A review. *Ecological Research, 19*, 119–129.
Bloom, D. E. (2011). 7 Billion and counting. *Science, 333*, 562–569.
Chapin, F. S., III, Zavaleta, E. S., Eviner, V. T., Naylor, R. L., Vitousek, P. M., Reynolds, H. L., ... Hobbie, S. E. (2000). Consequences of changing biodiversity. *Nature, 405*, 234–242.
Chen, Y., Li, X., Wang, S., & Liu, X. (2012). Defining agents' behaviour based on urban economic theory to simulate complex urban residential dynamics. *International Journal of Geographical Information Science, 26*, 1155–1172.
Chen, M., Liu, W., & Tao, X. (2013). Evolution and assessment on China's urbanization 1960–2010: under-urbanization or over-urbanization? *Habitat International, 38*, 25–33.
Chen, Y., Li, X., Liu, X., & Ai, B. (2014). Modeling urban land-use dynamics in a fast developing city using the modified logistic cellular automaton with a patch-based simulation strategy. *International Journal of Geographical Information Science, 28*(2), 234–255.
Chen, Y., Li, X., Liu, X., Ai, B., & Li, S. (2016). Capturing the varying effects of driving forces over time for the simulation of urban growth by using survival analysis and cellular automata. *Landscape & Urban Planning, 152*, 59–71.
Clarke, K. C., & Gaydos, L. J. (1998). Loose-coupling a cellular automaton model and GIS: Long-term urban growth prediction for San Francisco and Washington/Baltimore. *International Journal of Geographical Information Science, 12*, 699–714.
Costanza, R., & Ruth, M. (1998). Using dynamic modeling to scope environmental problems and build consensus. *Environmental Management, 22*, 183–195.
Coyle, R. G. (1997). System dynamics modelling: A practical approach. *Journal of the Operational Research Society, 48*, 544.
De Koning, G. H., Verburg, P. H., Veldkamp, A., & Fresco, L. O. (1999). Multi-scale modelling of land use change dynamics in Ecuador. *Agricultural Systems, 61*, 77–93.
Dietzel, C., & Clarke, K. C. (2007). Toward optimal calibration of the SLEUTH land use change model. *Transactions in GIS, 11*, 29–45.
Estoque, R. C., & Murayama, Y. (2012a). Examining the potential impact of land use/cover changes on the ecosystem services of Baguio city, the Philippines: A scenario-based analysis. *Applied Geography, 35*(1–2), 316–326.
Estoque, R. C., & Murayama, Y. (2012b). Introducing new measures of accuracy for land-use/cover change modeling. *Tsukuba Geoenvironmental Sciences, 8*, 3–7.
Foley, J. A., DeFries, R., Asner, G. P., Barford, C., Bonan, G., Carpenter, S. R., ... Gibbs, H. K. (2005). Global consequences of land use. *Science, 309*, 570–574.
Fu, B., Liu, G., Chen, L., Ma, K., & Li, J. (2001). Scheme of ecological regionalization in China. *Acta Ecologica Sinica, 21*(1), 1–6 [In Chinese].
Geist, H. J., & Lambin, E. F. (2004). Dynamic causal patterns of desertification. *Bioscience, 54*, 817–829.
Gustafson, E. J., Shifley, S. R., Mladenoff, D. J., Nimerfro, K. K., & He, H. S. (2000). Spatial simulation of forest succession and timber harvesting using LANDIS. *Canadian Journal of Forest Research, 30*, 32–43.
Haghani, A., Lee, S. Y., & Byun, J. H. (2003). A system dynamics approach to land use/transportation system performance modeling part I: Methodology. *Journal of Advanced Transportation, 37*, 1–41.
Hanley, J. A., & McNeil, B. J. (1982). The meaning and use of the area under a receiver operating characteristic (ROC) curve. *Radiology, 143*, 29–36.
Hansen, H. S. (2010). Modelling the future coastal zone urban development as implied by the IPCC SRES and assessing the impact from sea level rise. *Landscape and Urban Planning, 98*, 141–149.
Hay, J., & Mimura, N. (2006). Supporting climate change vulnerability and adaptation assessments in the Asia-Pacific region: An example of sustainability science. *Sustainability Science, 1*, 23–35.
He, C., Shi, P., Chen, J., Li, X., Pan, Y., Li, J., ... Li, J. (2005). Developing land use scenario dynamics model by the integration of system dynamics model and cellular automata model. *Science in China Series D: Earth Sciences, 48*, 1979–1989.
Heistermann, M., Müller, C., & Ronneberger, K. (2006). Land in sight? Achievements, deficits and potentials of continental to global scale land-use modeling. *Agriculture, Ecosystems & Environment, 114*, 141–158.
Huang, K., Liu, X., Li, X., Liang, J., & He, S. (2013). An improved artificial immune system for seeking the Pareto front of land-use allocation problem in large areas. *International Journal of Geographical Information Science, 27*, 922–946.
Huang, Q., He, C., Liu, Z., & Shi, P. (2014). Modeling the impacts of drying trend scenarios on land systems in northern China using an integrated SD and CA model. *Science China Earth Sciences, 57*, 839–854.
Kalnay, E., & Cai, M. (2003). Impact of urbanization and land-use change on climate. *Nature, 423*, 528–531.
Kline, J. D., Moses, A., Lettman, G. J., & Azuma, D. L. (2007). Modeling forest and range land development in rural locations: With examples from eastern Oregon. *Landscape and Urban Planning, 80*, 320–332.
Kok, K., & Winograd, M. (2002). Modelling land-use change for Central America: With special reference to the impact of hurricane Mitch. *Ecological Modelling, 149*, 53–69.
Lambin, E. F., Geist, H. J., & Lepers, E. (2003). Dynamics of land-use and land-cover change in tropical regions. *Annual Review of Environment and Resources, 28*, 205–241.
Letourneau, A., Verburg, P. H., & Stehfest, E. (2012). A land-use systems approach to represent land-use dynamics at continental and global scales. *Environmental Modelling & Software, 33*, 61–79.
Li, X., & Yeh, A. G. (2000). Modelling sustainable urban development by the integration of constrained cellular automata and GIS. *International Journal of Geographical Information Science, 14*, 131–152.
Li, X., & Yeh, A. G. (2002). Neural-network-based cellular automata for simulating multiple land use changes using GIS. *International Journal of Geographical Information Science, 16*, 323–343.
Li, X., Chen, Y., Liu, X., Li, D., & He, J. (2011). Concepts, methodologies: And tools of an integrated geographical simulation and optimization system. *International Journal of Geographical Information Science, 25*, 633–655.
Li, X., Lin, J., Chen, Y., Liu, X., & Ai, B. (2013). Calibrating cellular automata based on landscape metrics by using genetic algorithms. *International Journal of Geographical Information Science, 27*, 594–613.
Li, X., Guangzhao, C., Xiaoping, L., & Xun, L. (2017). Wang Shaojian A new global land-use and land-cover change product at a 1-km resolution for 2010–2100 based on human-environment interactions. *Annals of the Association of American Geographers, 107*(5), 1040–1059.
Liu, X., Li, X., Liu, L., He, J., & Ai, B. (2008). A bottom-up approach to discover transition rules of cellular automata using ant intelligence. *International Journal of Geographical Information Science, 22*, 1247–1269.
Liu, X., Li, X., Shi, X., Wu, S., & Liu, T. (2008). Simulating complex urban development using kernel-based non-linear cellular automata. *Ecological Modelling, 211*, 169–181.
Liu, X., Li, X., Shi, X., Zhang, X., & Chen, Y. (2010). Simulating land-use dynamics under planning policies by integrating artificial immune systems with cellular automata. *International Journal of Geographical Information Science, 24*, 783–802.
Liu, X., Ma, L., Li, X., Ai, B., Li, S., & He, Z. (2014). Simulating urban growth by integrating landscape expansion index (LEI) and cellular automata. *International Journal of Geographical Information Science, 28*, 148–163.
Liu, X., Hu, G., Ai, B., Li, X., Tian, G., Chen, Y., & Li, S. (2017). Simulating urban dynamics in China using a gradient cellular automata model based on S-shaped curve evolution characteristics. *International Journal of Geographical Information Science, 0*, 1–29.
Matson, P. A., Parton, W. J., Power, A. G., & Swift, M. J. (1997). Agricultural intensification and ecosystem properties. *Science, 277*, 504–509.
Mendelsohn, R., & Dinar, A. (1999). Climate change, agriculture, and developing countries: Does adaptation matter? *The World Bank Research Observer, 14*, 277–293.
Okin, G. S., Murray, B., & Schlesinger, W. H. (2001). Degradation of sandy arid shrubland environments: Observations, process modelling: And management implications. *Journal of Arid Environments, 47*, 123–144.
Openshaw, S. (1998). Neural network, genetic, and fuzzy logic models of spatial interaction. *Environment and Planning A, 30*, 1857–1872.
Pielke, R. A., Marland, G., Betts, R. A., Chase, T. N., Eastman, J. L., Niles, J. O., & Running, S. W. (2002). The influence of land-use change and landscape dynamics on the climate system: Relevance to climate-change policy beyond the radiative effect of greenhouse gases. *Philosophical Transactions of the Royal Society of London A: Mathematical Physical and Engineering Sciences, 360*, 1705–1719.
Pijanowski, B. C., Alexandridis, K. T., & Mueller, D. (2006). Modelling urbanization patterns in two diverse regions of the world. *Journal of Land Use Science, 1*, 83–108.
Pontius, R. G., Jr, & Millones, M. (2011). Death to Kappa: Birth of quantity disagreement and allocation disagreement for accuracy assessment. *International Journal of Remote Sensing, 32*, 4407–4429.
Pontius, R. G., Boersma, W., Castella, J., Clarke, K., de Nijs, T., Dietzel, C., ... Verburg, P. H. (2008). Comparing the input, output, and validation maps for several models of land change. *The Annals of Regional Science, 42*, 11–137.
Sala, O. E., Chapin, F. S., Armesto, J. J., Berlow, E., Bloomfield, J., Dirzo, R., ... Kinzig, A. (2000). Global biodiversity scenarios for the year 2100. *Science, 287*, 1770–1774.
Schaldach, R., Alcamo, J., Koch, J., Kölking, C., Lapola, D. M., Schüngel, J., ... Priess, J. A. (2011). An integrated approach to modelling land-use change on continental and global scales. *Environmental Modelling & Software, 26*, 1041–1051.
Schulp, C. J., Nabuurs, G., & Verburg, P. H. (2008). Future carbon sequestration in Europe—effects of land use change. *Agriculture Ecosystems & Environment, 127*, 251–264.
Sohl, T. L., Sayler, K. L., Drummond, M. A., & Loveland, T. R. (2007). The FORE-SCE

model: A practical approach for projecting land cover change using scenario-based modeling. *Journal of Land Use Science, 2*, 103–126.
Sohl, T. L., Sleeter, B. M., Sayler, K. L., Bouchard, M. A., Reker, R. R., Bennett, S. L., ... Zhu, Z. (2012). Spatially explicit land-use and land-cover scenarios for the Great Plains of the United States. *Agriculture, Ecosystems & Environment, 153*, 1–15.
Syphard, A. D., Clarke, K. C., & Franklin, J. (2007). Simulating fire frequency and urban growth in southern California coastal shrublands, USA. *Landscape Ecology, 22*, 431–445.
Tangen, K. (1999). The climate change negotiations: Buenos Aires and beyond. *Global Environmental Change, 9*, 175–178.
Tilman, D., Fargione, J., Wolff, B., D'Antonio, C., Dobson, A., Howarth, R., ... Swackhamer, D. (2001). Forecasting agriculturally driven global environmental change. *Science, 292*, 281–284.
Van Asselen, S., & Verburg, P. H. (2013). Land cover change or land-use intensification: Simulating land system change with a global-scale land change model. *Global Change Biology, 19*, 3648–3667.
Verburg, P. H., & Overmars, K. P. (2009). Combining top-down and bottom-up dynamics in land use modeling: Exploring the future of abandoned farmlands in Europe with the Dyna-CLUE model. *Landscape Ecology, 24*, 1167–1181.
Verburg, P. H., Soepboer, W., Veldkamp, A., Limpiada, R., Espaldon, V., & Mastura, S. S. (2002). Modeling the spatial dynamics of regional land use: The CLUE-S model. *Environmental Management, 30*, 391–405.
Verburg, P. H., Schot, P. P., Dijst, M. J., & Veldkamp, A. (2004). Land use change modelling: current practice and research priorities. *GeoJournal, 61*, 309–324.
Verburg, P. H., Schulp, C. J. E., Witte, N., & Veldkamp, A. (2006). Downscaling of land use change scenarios to assess the dynamics of European landscapes. *Agriculture Ecosystems & Environment, 114*, 39–56.
Vitousek, P. M., Mooney, H. A., Lubchenco, J., & Melillo, J. M. (1997). Human domination of Earth's ecosystems. *Science, 277*, 494–499.
Wang, F. (1994). The use of artificial neural networks in a geographical information system for agricultural land-suitability assessment. *Environment and Planning A, 26*, 265–284.
Ward, D. P., Murray, A. T., & Phinn, S. R. (2000). A stochastically constrained cellular model of urban growth. *Computers Environment and Urban Systems, 24*, 539–558.
White, R., Engelen, G., & Uljee, I. (1997). The use of constrained cellular automata for high-resolution modelling of urban land-use dynamics. *Environment and Planning B: Planning and Design, 24*, 323–343.
Wolf, J., Bindraban, P. S., Luijten, J. C., & Vleeshouwers, L. M. (2003). Exploratory study on the land area required for global food supply and the potential global production of bioenergy. *Agricultural Systems, 76*, 841–861.
Wu, F. (1999). GIS-based simulation as an exploratory analysis for space-time processes. *Journal of Geographical Systems, 1*, 199–218.
Wu, F. (2002). Calibration of stochastic cellular automata: The application to rural-urban land conversions. *International Journal of Geographical Information Science, 16*(8), 795–818.
Xiang, W., & Clarke, K. C. (2016). The use of scenarios in land-use planning. *Environment and Planning B: Planning and Design, 30*(6), 885–909.
Yao, Y., Li, X., Liu, X., Liu, P., Liang, Z., Zhang, J., Mai, K., ... (2016). Sensing spatial distribution of urban land use by integrating points-of-interest and Google Word2Vec model. *International Journal of Geographical Information Science,* 1–24.